

In situ MAS NMR investigations of molecular sieves and zeolite-catalyzed reactions

Eric G. Derouane^{a,*}, Heyong He^a, Sharifah Bee Derouane-Abd Hamid^a and Irina I. Ivanova^b

^a Leverhulme Centre for Innovative Catalysis, Department of Chemistry, The University of Liverpool, PO Box 147, Liverpool L69 3BX, UK
E-mail: derouane@liverpool.ac.uk

^b Department of Chemistry, Moscow State University, Vorobievsky Gory, 119899 Moscow, Russia

Received 17 August 1998; accepted 19 January 1999

Solid-state MAS NMR is a powerful technique to study heterogeneous catalysts and the way by which they operate. *In situ* MAS NMR has been demonstrated to be a powerful method to understand reaction mechanisms, to study the nature, dynamics and reactivity of surface intermediates and active sites, and to characterize structural modifications in the catalyst itself, in particular when using ¹³C strategically labelled substrates. In this paper, three examples selected from our own work are used to illustrate the potential of *in situ* MAS NMR. They are the formation of cumene and its isomerization to *n*-propylbenzene on zeolite H-ZSM-11, the activation of propane at low temperature and the alkylation of benzene with propane on zeolite H-ZSM-5, and the characterization of the aluminophosphate molecular sieve VPI-5 structure with temperature. Studies of the alkylation of benzene with propene confirmed that cumene was the primary reaction product. The undesired *n*-propylbenzene by-product results from the intermolecular reaction between cumene and benzene, enhanced by molecular shape-selective effects in medium pore size zeolites (e.g., H-ZSM-11). It explains why large pore zeolites, e.g., zeolite Beta, are used commercially today for this process. Propane can be activated at low temperature (ca. 573 K) on bifunctional medium pore size zeolites possessing intimately related acidic Brønsted sites and a dehydrogenation function provided by Ga or Zn species. In Ga/H-ZSM-5 catalysts, at 573 K, the activation of propane was shown to occur via a protonated pseudocyclopropane (PPCP) intermediate (or transition state). The latter evolves in a manner that can be formally described by the formation of CH₃⁺, C₂H₅⁺, and C₃H₇⁺ carbenium ion intermediates. These species can react with olefins, alkanes, or other electron-rich molecules such as benzene. The primary reaction products of the reaction of propane with benzene are *n*-propylbenzene (in small amount), ethylbenzene and toluene. Their subsequent reactions lead eventually to toluene and xylenes as the final products. In the structural characterization of VPI-5, ²⁷Al, ³¹P, and ²⁷Al nutation MAS NMR spectra show that, at 294 K, fully hydrated VPI-5 contains three equally populated Al and P crystallographic sites and that one-third of Al is 6-coordinate. The VPI-5 structure then belongs to the P6₃ space group. Above 353 K, VPI-5, fully or partially hydrated, undergoes a structural transformation to a higher framework symmetry, i.e., the P6₃cm space group. The transformation occurs at nearly the same temperature in both cases, indicating that the breakdown of the hydrogen-bonded helical water structure inside the VPI-5 pores is not a factor in the process.

Keywords: zeolites, chemicals, NMR, alkane activation, reaction mechanism, *in situ* investigation, alkylation

1. Introduction

Solid-state MAS NMR spectroscopy has been widely used for the characterization of molecular sieves and other heterogeneous catalysts [1–3]. Unique and important structural information that cannot be derived from other techniques, such as X-ray diffraction (XRD), may be obtained from solid-state NMR measurements. For example, MAS NMR can provide information on distinct local orderings in solids whereas XRD measurements yield only their averages. MAS NMR is currently one of the most important techniques for the structural characterization of catalytic materials.

In situ MAS NMR has also been applied to study reaction mechanisms in heterogeneous catalysis [4,5] and it has greatly contributed to our fundamental understanding of catalyst behavior and catalytic processes. *In situ* MAS NMR means here that measurements are performed in con-

ditions mimicking actual catalysis. They are usually made in batch-like conditions, the nature of the components in the sealed NMR cell being controlled initially and subsequently monitored as the reaction proceeds.

Heterogeneous catalytic reactions involving organic molecules are conventionally followed by analyzing the reactor effluent that contains the reactant(s), the reaction intermediate(s), and the product(s). Reaction mechanisms are indirectly inferred from kinetics equations derived by varying experimental variables such as temperature, pressure, flow rates, contact time, etc. To fully understand and prove these reaction mechanisms and to obtain additional information on the role and dynamics of the active sites, it is necessary to analyze the reactants, intermediates and products in the adsorbed state and to qualify their interaction with the active sites.

Except FT-IR and FT-Raman, commercial *in situ* spectroscopic instrumentation is still not widely available today. As most heterogeneous catalysts are porous materials, sur-

* To whom correspondence should be addressed.

face electron spectroscopies have limited application to the study of bulk heterogeneous catalysts. Although *in situ* powder XRD is best suited for the determination of the catalyst structural changes during reaction, it is blind to organic molecules which have no long-range order in the catalyst. IR and Raman spectroscopies detect these organic molecules but, most often, the quantification of the data is complicated by the existence of overlapping absorption peaks and uncertainties in the values of the substrate extinction coefficients. In contrast, ^{13}C NMR spectroscopy enables the differentiation of different organic compounds as almost every organic compound has its individual chemical shift(s) “fingerprints”. NMR is also quantitative as it actually counts nuclear spins.

The two main advantages of *in situ* MAS NMR performed in batch-like conditions are thus obvious. The use of sealed ampoules allows (i) the full quantification of the reaction mixture of which the composition can be established on the basis of the observed chemical shifts and (ii) the extensive and rather economical use of strategically labelled reactants, enabling detailed mechanistic investigations.

NMR resonance lines are much broader for solids than for liquids due to the net anisotropy interaction resulting from chemical shift anisotropy, dipole–dipole and quadrupolar interactions. The mobility of molecules adsorbed in heterogeneous catalysts is reduced significantly by the interactions between the adsorbed molecules and the catalyst surface and adsorbed molecules themselves. They thus show also broad NMR lines in normal conditions. The NMR linewidth corresponding to adsorbed species is however noticeably reduced when the sample is spun at high frequency (up to 30 kHz) and at an angle of 54.74° relative to the external magnetic field, a technique called magic-angle spinning (MAS) NMR. In addition, nearly all molecules are adsorbed at sufficiently low temperature (this is certainly true for organic compounds in zeolites at ambient temperature), which enables the quantification of the reaction mixture.

In situ MAS NMR is thus most suitable to follow reaction pathways by identifying reaction intermediates in the adsorbed state. When using strategically ^{13}C -labelled compounds, it enables to study quantitatively the behaviour of specific molecules with some advantage relative to the more conventional GC-MS analysis of downstream vapours (GC-MS usually requires a detailed and sometime tedious analysis of the labelled atom distribution). When applying *in situ* MAS NMR, the catalyst and the reactants are either sealed in a well-balanced glass cell which perfectly fits in the MAS rotor in order to achieve a sufficiently high spinning rate (3–4 kHz) or are simply sealed in the NMR rotor with special caps [6–13]. The NMR cell is exposed to reaction conditions at different pressures, temperatures and time lengths, and the reaction is quenched in liquid nitrogen for CA MAS NMR observation at room temperature. *In situ* MAS NMR performed in batch-like conditions is flexible,

quantitative, and rather economical in terms of ^{13}C label compounds utilization.

We will not discuss in this paper flow-through *in situ* NMR techniques and experiments in which the NMR cell is exposed to a continuous flow of reactants. More than 10 years ago, Haddix et al. designed a static *in situ* flow probe mimicking a bench-top flow reactor [14,15]. More recently, different designs of *in situ* MAS NMR flow probes have been proposed by Hunger et al. [16,17] and Haw et al. [18–20]. Despite their elegance and advantage to operate in truly real conditions, the application of such designs may be restricted by the high costs of ^{13}C -labelled reactants needed in a flow system. Nevertheless, they prove that fully *in situ* MAS NMR is also available today and there is no doubt that rapid progress will be made in its development and applications.

The aim of this paper is to demonstrate by examples selected from our own work [21–31] that *in situ* MAS NMR in batch-like conditions, as applied to heterogeneous catalysis, contributes greatly to the detailed understanding of reaction mechanisms, the identification of reaction intermediates and of their interaction with catalytic sites, and the characterization of structural transformations in potential catalytic materials.

The examples which we have selected are:

1. The reaction of benzene with propene, catalyzed by H-ZSM-11: cumene and *n*-propylbenzene are formed as primary and secondary product, respectively.
2. The low-temperature activation of propane on a bifunctional Ga/H-ZSM-5 catalyst: a protonated pseudocyclopropane intermediate has been identified which shows reactivity towards olefins, alkanes, and electron-rich molecules.
3. The temperature-dependent crystallographic transformation of the aluminophosphate molecular sieve VPI-5.

2. Experimental

2.1. ^{13}C CA MAS NMR studies

The H-ZSM-11, H-ZSM-5, Ga/H-ZSM-5, and NaY zeolite catalysts were synthesized using recipes well-documented in the literature and described in our original publications [21–31].

Propene-1- ^{13}C (99.9%, ^{13}C), isopropanol-2- ^{13}C (99.9%, ^{13}C), and benzene (5%, ^{13}C) were obtained from MSD Isotopes. Propane-2- ^{13}C (99.9%, ^{13}C) and propene-2- ^{13}C (99.9%, ^{13}C) were obtained from ICON Services Inc. Propene-2- ^{13}C (99.9%, ^{13}C) was also prepared at 623 K by dehydration of isopropanol-2- ^{13}C (99.9%, ^{13}C) on zeolite NaY with 100% conversion and selectivity. Cumene with ^{13}C in β -position of the alkyl chain and in the aromatic ring was synthesized directly in the NMR cell over

Table 1
Catalysts used in the controlled atmosphere MAS NMR study of catalytic reaction mechanisms.

Reaction	Catalyst
Cumene formation and isomerization to <i>n</i> -propylbenzene	H-ZSM-11 (Si/Al = 25)
Activation of propane at low temperature	Ga/silicalite (Si/Al = 480, 0.96 wt% Ga) Ga/H-ZSM-5 (Si/Al = 35, 1.02 wt% Ga) H-ZSM-5 (Si/Al = 35, 63, 480)
Benzene alkylation with propane	Ga/H-ZSM-5 (Si/Al = 35, 0.95 wt% Ga)

Table 2
Sample preparation for cumene synthesis and isomerization to *n*-propylbenzene.

Experiment ^a	Catalyst	Loaded reactant (molec./u.c.)					
		C ₆ H ₆	C ₆ H ₆ - (1-6)- ¹³ C	C ₃ H ₆ - 1- ¹³ C	C ₃ H ₆ - 2- ¹³ C	Cumene- (1-6, β)- ¹³ C	Cumene
A	H-ZSM-11	9	–	–	1	–	–
B	H-ZSM-11	9	–	1	–	–	–
B'	H-ZSM-11	9	–	1	–	–	–
C	H-ZSM-11	9	–	9	–	–	–
D	H-ZSM-11	8	–	–	–	4	–
E	H-ZSM-11	–	8	–	–	–	4
F	Silylated H-ZSM-11	9	–	3	–	–	–

^a NMR cell volumes in experiments B' and A–F were 0.59 and 0.24 cm³, respectively.

Table 3
Sample preparation for propane activation at low temperature.

Experiment	Catalyst	Pretreatment ^a	Loaded reactant and additives (molec./u.c.)			
			C ₃ H ₈ -2- ¹³ C	H ₂ O	CO	C ₃ H ₆
1	Ga/H-ZSM-5(35)	A	4	–	–	–
2	Ga/H-ZSM-5(480)	A	4	–	–	–
3	H-ZSM-5(63)	A	4	–	–	–
4	H-ZSM-5(35)	B	4	–	–	–
5	H-ZSM-5(35)	A	4	4	–	–
6	H-ZSM-5(35)	A	4	–	4	–
7	H-ZSM-5(35)	A	4	–	–	0.5

^a A: 573 K, 8 h; B: 790 K, 48 h.

H-ZSM-11 by benzene (5%, ¹³C) alkylation with propene-1-¹³C (99.9%, ¹³C) at room temperature with 100% yield and selectivity.

Tables 1–5 show the catalysts used in NMR study and sample preparations.

¹³C *in situ* MAS NMR spectra were recorded on Bruker CXP-200 or MSL-400 spectrometers at 50.3 and 100.6 MHz, respectively, with 90° pulses and 4 s recycle delays at a spinning rate of 2.5–4 kHz. Quantitative conditions were achieved using high-power gated proton decoupling with suppressed NOE effect. Some non-¹H-decoupling spectra were recorded to identify reaction products and intermediates. Cross-polarization experiments were performed to distinguish between species with different mobilities. Chemical shifts are given in ppm from external tetramethylsilane (TMS).

Powdered catalyst samples (0.07–0.10 g) were packed into NMR cells (Wilmad 5.6 mm o.d. with constrictions) fitting exactly into the double-bearing Bruker 7 mm zirconia rotors. The catalysts were evacuated to a pressure of 6×10^{-6} Torr after heating for 8 h at 573 K and cooled to 298 K before adsorption. Liquid reactants were dosed gravimetrically while gaseous reactants were dosed volumetrically. After introduction of the reactants, the NMR cells were immersed in liquid nitrogen to ensure quantitative adsorption and sealed.

In a typical experiment, the sealed NMR cell was rapidly heated to a selected temperature and maintained at this temperature for various duration of time. The MAS NMR spectra were recorded at 293 K after rapid quenching of the NMR sample cell in liquid nitrogen. After collection of the NMR data, the NMR cell was returned to reaction

Table 4
Characteristics of H-ZSM-5 catalysts for propane activation at low temperature.

Catalyst	Composition				Acidity			
	Si/Al chem.	Si/Al lattice ^a	Al _T /u.c.	Al _{ext} /u.c.	Catalyst pretreat. ^b	Br/L	Br/u.c. ^c	L/u.c. ^c
H-ZSM-5(480)	480	480	0.2	–	A	–	traces	–
H-ZSM-5(35)	35	35	2.5	–	A	11	2.3	0.2
					B	4	2.0	0.5
H-ZSM-5(35) modified	35	63	1.5	1.0	A	1.5	1.4	1.1

^a Determined by ²⁹Si MAS NMR.

^b A: 573 K, 8 h; B: 790 K, 48 h. Vacuum.

^c Br: Brønsted sites; L: Lewis sites; determined by FTIR of adsorbed pyridine; after desorption at 423 K.

Table 5
Sample preparation for benzene alkylation with propane.

Experiment	Catalyst	Loaded reactant (molec./u.c.)			
		Propane-2- ¹³ C	Benzene	H ₂	Cumene- α - ¹³ C
A	Ga/H-ZSM-5	–	9	3	–
B	Ga/H-ZSM-5	3	–	–	–
C	Ga/H-ZSM-5	3	9	–	–
D	Ga/H-ZSM-5	1	9	–	–
E	H-ZSM-5	–	6	–	3

conditions, heated for progressively longer periods of time or at higher temperature.

Conversion of reactant *r* at time *t* was determined as

$$X_{r,t} = (1 - I_{r,t}/I_{r,0}) \times 100 (\%),$$

where *I_{r,t}* is the integrated intensity of the reactant *r* resonance in the NMR spectrum after heating for time *t*; *I_{r,0}* is the integrated intensity of the reactant *r* resonance in the initial NMR spectrum.

Yield of product *p* at time *t* was determined as

$$Y_{p,t} = I_{p,t}/I_{r,0} \times 100 (\%),$$

where *I_{p,t}* is the integrated intensity of the product *p* resonance in the NMR spectrum after heating for time *t*.

2.2. Structural study of VPI-5

VPI-5 was synthesized with DPA and TBA as templates according to the optimized compositions established in [32]. Fully hydrated samples were obtained by exposing the materials in a desiccator for 12 h to the water vapor pressure of a saturated solution of NH₄Cl. To prepare a partially hydrated sample, VPI-5 was evacuated to a pressure of 10^{−4} Torr for two days and rehydrated for 24 h with 10% D₂O + 90% H₂O. The sample was then heated for ca. 15 min at 373 K, *in situ* in a NMR rotor with a hole in the cap until no intensity change was observed in the ²H NMR spectrum. For the NMR experiments, the sample was then transferred to a tightly closed rotor in a dry box.

²H, ²⁷Al, and ³¹P NMR spectra were recorded on a Bruker MSL-400 spectrometer at 61.4, 104.3 and 162.0 MHz,

respectively. ²H spectra were recorded using a quadrupole echo pulse sequence with a 20 μs echo delay and a 2 s recycle delay. ²⁷Al spectra were recorded with 0.6 μs (<10°) pulses and 0.3 s recycle delays with magic-angle-spinning at 10–12 kHz. ²⁷Al nutation spectra were recorded with ω_{rf}/2π of 115 ± 5 kHz and with magic-angle-spinning at 8–12 kHz. ³¹P spectra were recorded with 1 μs (30°) pulses and 30 s recycle delays with magic-angle-spinning at 7–12 kHz. Chemical shifts of ²H, ²⁷Al and ³¹P are given in ppm from external D₂O, Al(H₂O)₆³⁺ and 85% H₃PO₄, respectively.

3. Results and discussion

3.1. Alkylation of benzene with propylene: formation of cumene and isomerization of cumene to *n*-propylbenzene

Cumene is an important intermediate in the industrial production of phenol, acetone and α-methylstyrene. The formation of cumene on medium pore size zeolites, such as ZSM-5 and ZSM-11, is accompanied by its isomerization to *n*-propylbenzene. The latter is an undesired by-product with respect to further processing of cumene to phenol and acetone. Therefore, it is of interest to identify means or catalytic systems which suppress or minimize the isomerization of cumene to *n*-propylbenzene. Understanding the mechanisms of cumene formation and isomerization is obviously an important step in this direction.

When propene-2-¹³C or propene-1-¹³C are adsorbed on H-ZSM-11 in the presence of an excess of benzene (experiments A and B, table 2), a weak resonance is observed

at 128 ppm in both ^{13}C NMR spectra, corresponding to the aromatic carbons of benzene and cumene (^{13}C in natural abundance). The intense lines at 34 and 24 ppm are assigned to the α - ^{13}C and β - ^{13}C carbons of cumene, respectively. No other resonances, including those identifying propene are observed, indicating the rapid and complete reaction of propene with benzene at 298 K.



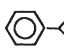



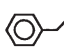


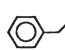


The absence of broad lines in the range of 14–40 ppm, corresponding to oligomerization products, suggests the suppression of the competitive oligomerization of propene in the presence of benzene in large excess. Benzene traps and reacts selectively with the propenium ions formed from propene. This conclusion is supported by the actual observation of such broad resonances at ca. 14 and 30 ppm, assigned to propene oligomers, when equimolar amounts of propene-1- ^{13}C and benzene are adsorbed and reacted (experiment C, table 2). Upon heating to 413 K, a new resonance appears at ca. 40 ppm, suggesting isomerization and ^{13}C scrambling in oligomers. Eventually, further heating results in cracking of the oligomers and alkylation of benzene with the fragments. Weak resonances corresponding to cumene α - ^{13}C and *sec*-butylbenzene are observed.

According to classical concepts [33,34], alkylation of an aromatic ring by an olefin occurs via olefin protonation and subsequent electrophilic attack of the carbenium ion on the aromatic π -system, yielding a benzenium cation that can re-aromatize by proton loss. The formation of carbenium ion is believed to be the rate-limiting step. Our tracing of the 1- ^{13}C and 2- ^{13}C carbon atom of propene when alkylating benzene on H-ZSM-11 is in line with the classical carbenium ion mechanism, but the nature of the rate-limiting step is questionable. Indeed, extremely rapid alkylation at 298 K in the adsorbed phase contrasts with the significantly higher temperature (ca. 473 K) required when the reaction is conducted in the liquid phase [35]. It suggests that desorption and diffusion of the product(s) may be rate limiting in liquid phase when the temperature is too low. Rapid catalyst deactivation at 473 K confirms this [35]. Our results also explain the formation of noticeable amounts of *sec*-butylbenzene when benzene is alkylated with propene in flow conditions and at comparatively low temperature [35,36].

The classical mechanism for alkylation implies carbenium ion intermediates. However, the existence of free carbenium ions of non-branched light olefins is rather doubtful [9,36,37]. They are most likely present as alkoxy species resulting from their binding to oxygen anions adjacent to aluminium sites in the zeolite framework or, in simpler words, reaction of an olefin with a zeolite Brønsted site yields a surface alkoxy species. A concerted mechanism including the formation and subsequent decomposition of surface alkoxy groups was proposed for oligomerization and bond shift reactions [38]. The transition state in this mechanism has a cationic character and all the rules of the classical carbenium ion formalism must therefore also be obeyed.

Table 6

Effect of the isomerization mechanism and of the initial ^{13}C label position in the aromatic rings of cumene and benzene, on the ^{13}C label distribution in resulting *n*-propylbenzene and benzene.

Reagents	 + 	 + 
Mechanism		
INTRA	 + 	 + 
INTER	 + 	 + 

● indicates ^{13}C -labelled carbon atom.

As mentioned earlier, a major side-reaction of cumene synthesis is its isomerization to undesired *n*-propylbenzene. Several investigations of the isomerization of cumene over acid catalysts [39–44] suggest that both inter- and intra-molecular pathways may occur depending on catalysts and reaction conditions. Strategic ^{13}C labelling of the reactants is ideal to resolve this controversy.

As shown in table 6, two simple experiments can be and were performed. One involves cumene, fully labelled on the aromatic ring (no label on the side chain), and unlabelled benzene (experiment D, table 2). The other is the reaction of unlabelled cumene with fully labelled benzene (experiment E, table 2). In the former case, the reaction products are labelled *n*-propylbenzene and unlabelled benzene if the process is intramolecular, and labelled benzene and unlabelled *n*-propylbenzene if the reaction is intermolecular. In the latter case, intramolecular conversion yields unlabelled *n*-propylbenzene and labelled benzene whereas an intermolecular process leads to unlabelled benzene and labelled *n*-propylbenzene. The key to interpret CA MAS NMR spectra for these experiments is the chemical shift characterizing the aromatic ring carbon atom (^{13}C -1) linked to the side chain: 128 ppm for benzene (no side chain), 149 ppm for cumene, and 142.5 ppm for *n*-propylbenzene.

When labelled cumene is reacted with unlabelled benzene (figure 1(a)), the spectrum of the unreacted sample shows three lines at 149, 128 and 126 ppm, corresponding to ^{13}C -1 in cumene, ^{13}C -3,5 in cumene and natural abundance ^{13}C in benzene, and ^{13}C -2,4,6 in cumene, respectively. After heating for 60 min, the conversion of cumene to *n*-propylbenzene, estimated from the aliphatic region of the spectrum, is more than 60%. The line at 149 ppm assigned to ^{13}C -1 in cumene disappears and the line at 142.5 ppm corresponding to ^{13}C -1 in *n*-propylbenzene is not observed. It suggests that the isomerization of cumene is intermolecular.

The counter-experiment with labelled benzene and unlabelled cumene (figure 1(b)) shows the appearance of a new resonance at 143 ppm. This observation confirms unambiguously the intermolecular character of isomerization of cumene in the presence of benzene. Next is the intimate understanding of the reaction mechanism.

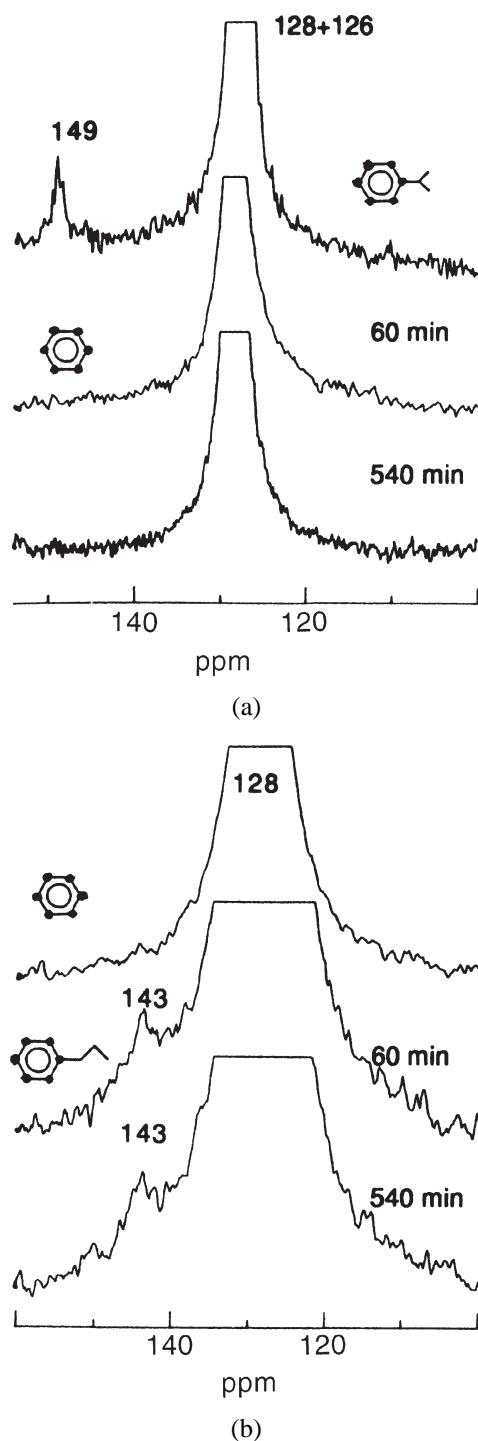


Figure 1. ^{13}C MAS NMR spectra of labelled cumene and unlabelled benzene (a) and labelled benzene and unlabelled cumene (b) before and after reaction over H-ZSM-11 at 473 K. Benzene/cumene = 2. • indicates ^{13}C -labelled carbon atom.

Transalkylation of alkylaromatics can proceed by either a $\text{S}_{\text{N}}1$ or a $\text{S}_{\text{N}}2$ mechanism, as shown in figure 2 [45,46]. The $\text{S}_{\text{N}}1$ mechanism implies the cleavage of an isopropyl group and the formation of a 2-propenium ion. To form *n*-propylbenzene by this mechanism, a 2-propenium cation must rearrange either to a less stable 1-propenium cation (mechanism (1a), figure 2) or to a cycloproponium ion with

intermediate stability (mechanism (1b), figure 2) [47,48]. Formation of *n*-propylbenzene by the $\text{S}_{\text{N}}2$ mechanism occurs via a 1,2-diphenyl-1-methylethane intermediate (mechanism (2), figure 2). The formation of the 1,2-diphenyl-1-methylethane intermediate also occurs via a primary cation, but this process may have a lower activation energy due to the resonance stabilization of the carbocation intermediate.

^{13}C in situ MAS NMR measurements using a ^{13}C label in the alkyl chain easily discriminate between mechanisms (1b) and (1a) or (2), as shown in table 7, since only mechanism (1b) should lead to a complete scrambling of the ^{13}C label. Mechanisms (1a) and (2) lead to similar distributions of the labels in the alkyl chain (50% on the α and γ carbon atoms). The chemical shifts of the alkyl chain carbon atoms are 34 ppm for α - ^{13}C and 24 ppm for β - ^{13}C in cumene, and 38 ppm for α - ^{13}C , 25 ppm for β - ^{13}C , and 14 for γ - ^{13}C in *n*-propylbenzene.

The isomerization of cumene- α - ^{13}C leads to a new resonance at 25 ppm characteristic of β - ^{13}C in *n*-propylbenzene (figure 3(a)). The counter-experiment with cumene- β - ^{13}C shows lines at 14 and 38 ppm only (figure 3(b)). Thus, mechanism (1a) or (2) is operative.

To discriminate further between the bimolecular $\text{S}_{\text{N}}2$ (mechanism (2)) and the monomolecular $\text{S}_{\text{N}}1$ (1a) mechanisms, the effect of pressure on the reaction rate was studied. Relative pressure was varied by changing the volume of the NMR sample cell, all other conditions being the same (samples B and B' in table 2). It was observed that the rate of isomerization increases non-linearly with pressure, indicating that must be bimolecular. Thus, cumene isomerization is intermolecular. It occurs via an intermolecular $\text{S}_{\text{N}}2$ pathway involving diphenylmethylethane as an intermediate. The only remaining question addresses the specific role of the zeolite acid catalyst, i.e., the possible role of molecular shape-selective effects.

To differentiate between the contributions of the external and internal surfaces of the zeolite to the reaction, the external surface of the H-ZSM-11 catalyst was passivated by silylation [49] (experiment F, table 2). The observed NMR spectra were qualitatively similar to those obtained on non-modified catalyst. Therefore, we conclude that the isomerization of cumene in medium pore size zeolites occurs inside the intracrystalline free space. This result agrees with the observation that isomerization of *para*-cymene to *n*-propyltoluene takes place inside the channels of zeolite ZSM-5 [50] and may contradict earlier conclusions [51].

Although the 1,2-diphenyl-1-methylethane intermediate looks rather bulky, molecular modelling shows that its cross section is close to that of cumene. Therefore, there are no serious restrictions to mechanism (2) (figure 2) taking place in zeolites such as H-ZSM-11 or H-ZSM-5, even more so when considering the additional space which is available at their three-dimensional channel intersections. Unfortunately, the steric constraints imposed by these materials pore structure favor the reaction between the β -carbon of the alkyl chain carbon of cumene with benzene yielding undesired *n*-propylbenzene.

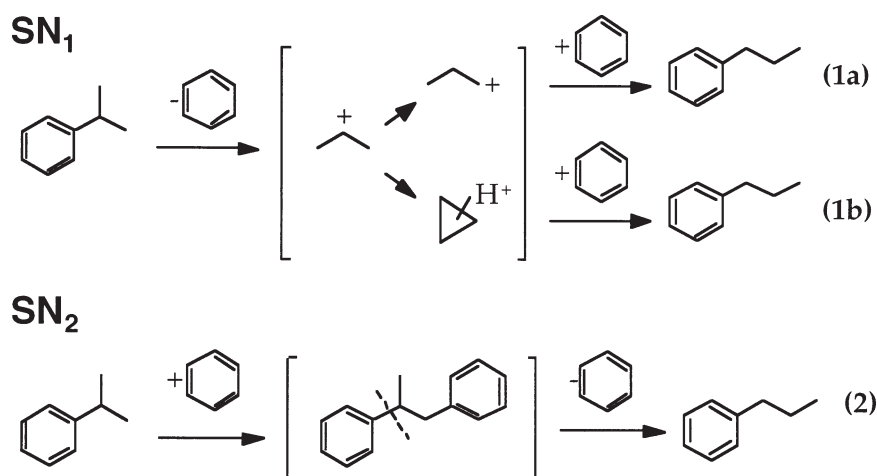


Figure 2. Intermolecular transalkylation pathways for cumene isomerization.

Table 7

Effect of the isomerization mechanism and of the initial ^{13}C label position in the aliphatic chain of cumene on the ^{13}C label distribution in resulting *n*-propylbenzene.

Reactant			
Mechanism			
1(a)	100%	50%	50%
1(b)	33%	33%	33%
2	100%	50%	50%

• indicates ^{13}C -labelled carbon atom.

Intermolecular transalkylation can occur via the bulkier 2,2-diphenylpropane intermediate (the preferred route in terms of carbenium ion chemistry) in large pore zeolites such as MOR and BEA, in which case the original reactants are restored. This means that large pore size zeolites are preferred catalysts for cumene production, a commercial reality today but still an open question when this research was initiated.

In conclusion, *in situ* MAS NMR experiments show unambiguous evidence for a carbenium ion mechanism in cumene formation. Competition between alkylation and oligomerization occurs at low benzene to propene ratio. The primary alkylation product is cumene which is isomerized to *n*-propylbenzene via an S_N2 intermolecular mechanism in medium pore size zeolites such as ZSM-5 or ZSM-11. Large pore size zeolites such as zeolite Beta or Y are thus preferred catalysts for the production of cumene.

3.2. ^{13}C *in situ* MAS NMR investigation of propane activation at low temperature on Ga/H-ZSM-5

The activation and functionalization of light alkanes receive increasing attention because of the need to find commercially attractive routes for using economical alkanes

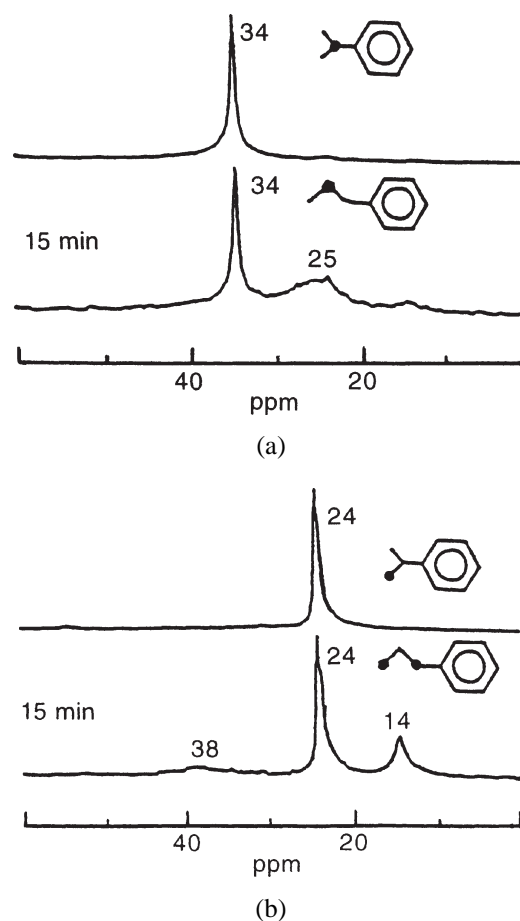


Figure 3. ^{13}C MAS NMR spectra observed before and after reaction of cumene with benzene over H-ZSM-11 at 473 K: cumene α - ^{13}C (a) or cumene β - ^{13}C (b) with benzene (benzene/cumene = 8). • indicates ^{13}C -labelled carbon atom.

feeds to replace other more costly reactants such as olefinic or aromatic compounds.

The aromatization of propane on acidic zeolite catalysts has been widely discussed. The attention was focused mainly on zeolite H-ZSM-5, usually modified by the addition of a dehydrogenation component involving elements

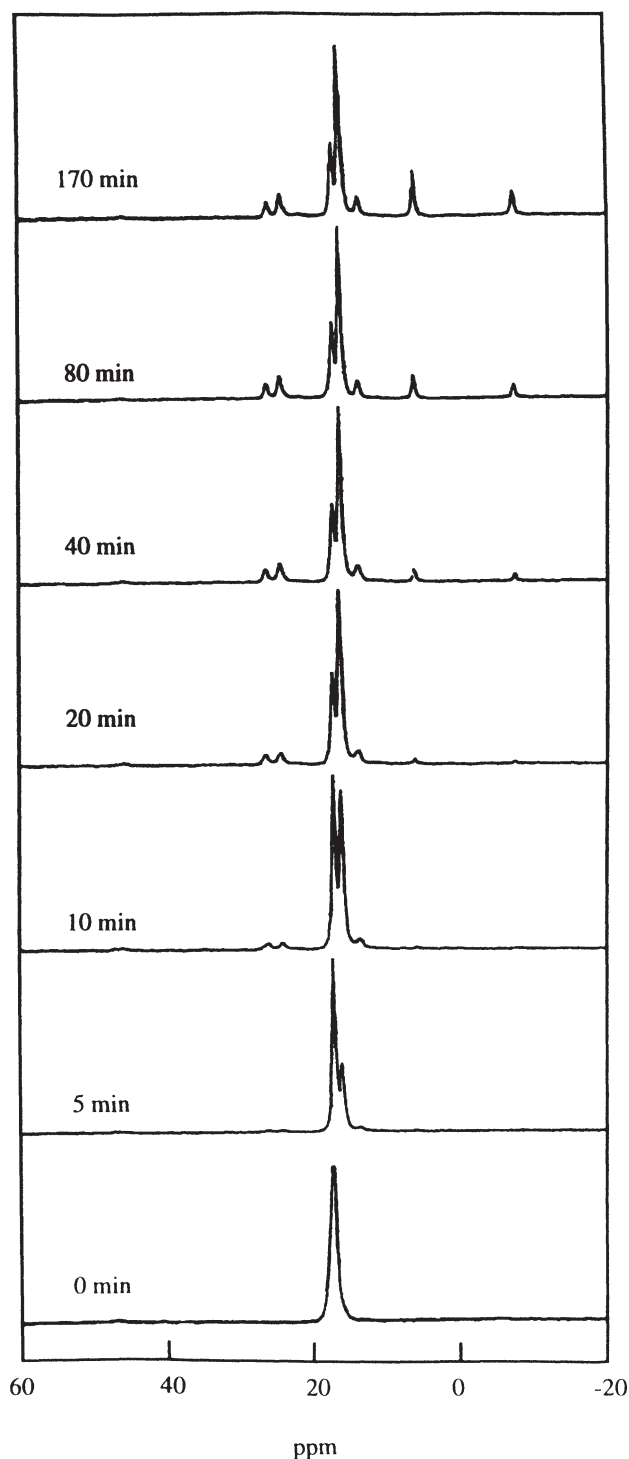


Figure 4. ^{13}C MAS NMR spectra observed after reaction of propane-2- ^{13}C (4 molecules/u.c.) at 573 K on Ga/H-ZSM-5 (Si/Al = 35).

such as Ga and Zn as oxides. Ga/H-ZSM-5 is the preferred catalyst [52–64] used in a commercial process, CYCLAR, which is now jointly developed commercially by UOP and BP. Aromatization is generally achieved at a temperature in the range 773–823 K and its pathway has been extensively described in the literature. In contrast, the mechanism responsible for the activation of propane at low temperature still remains a source of controversy.

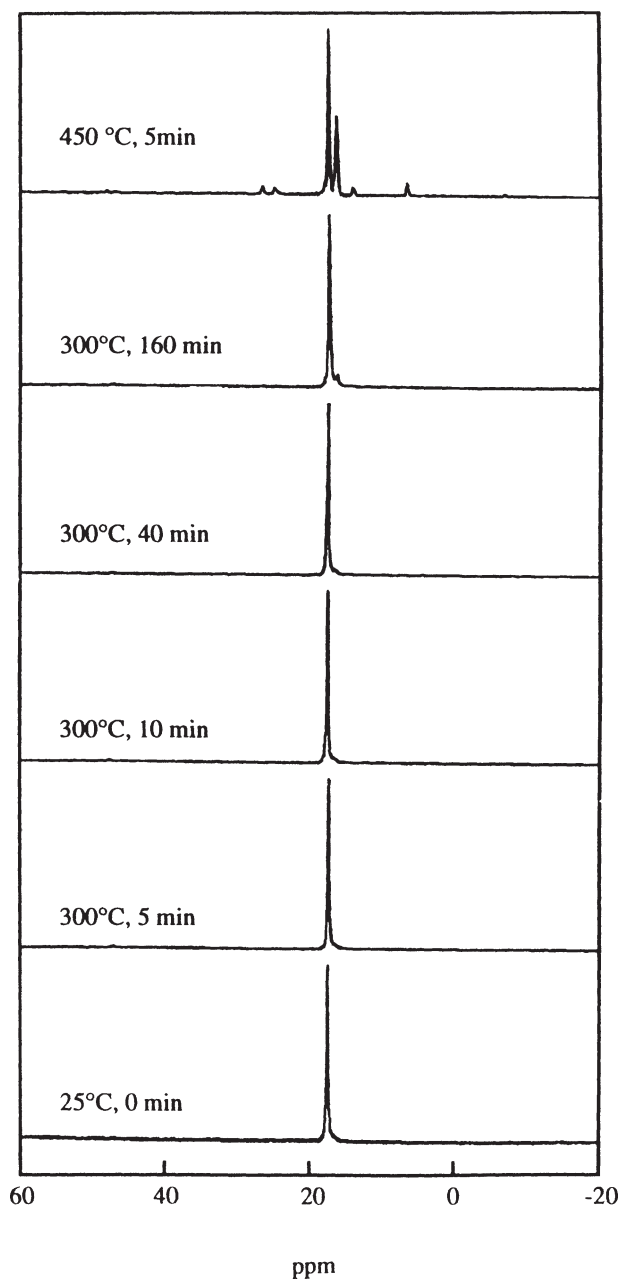


Figure 5. ^{13}C MAS NMR spectra observed after reaction of propane-2- ^{13}C (4 molecules/u.c.) on Ga/silicalite at 573 and 723 K (Si/Al = 480).

We have addressed this problem by using ^{13}C *in situ* MAS NMR using strategically labelled propane-2- ^{13}C as reactant. Table 3 lists the experiments which were performed and tables 1 and 4 give the characteristics of the catalysts. Three experiments using Ga/silicalite, Ga/H-ZSM-5, and H-ZSM-5 were performed to investigate the synergistic action of the dehydrogenation function provided by the gallium species and the Brønsted acidic sites of the zeolite.

The reaction of propane on Ga/H-ZSM-5 begins at 573 K. Typical spectra showing its progressive transformation on a Ga/H-ZSM-5 (Si/Al = 35, experiment 1 in table 3) are shown in figure 4. The initial spectrum shows only a resonance at ca. 17 ppm, corresponding to the la-

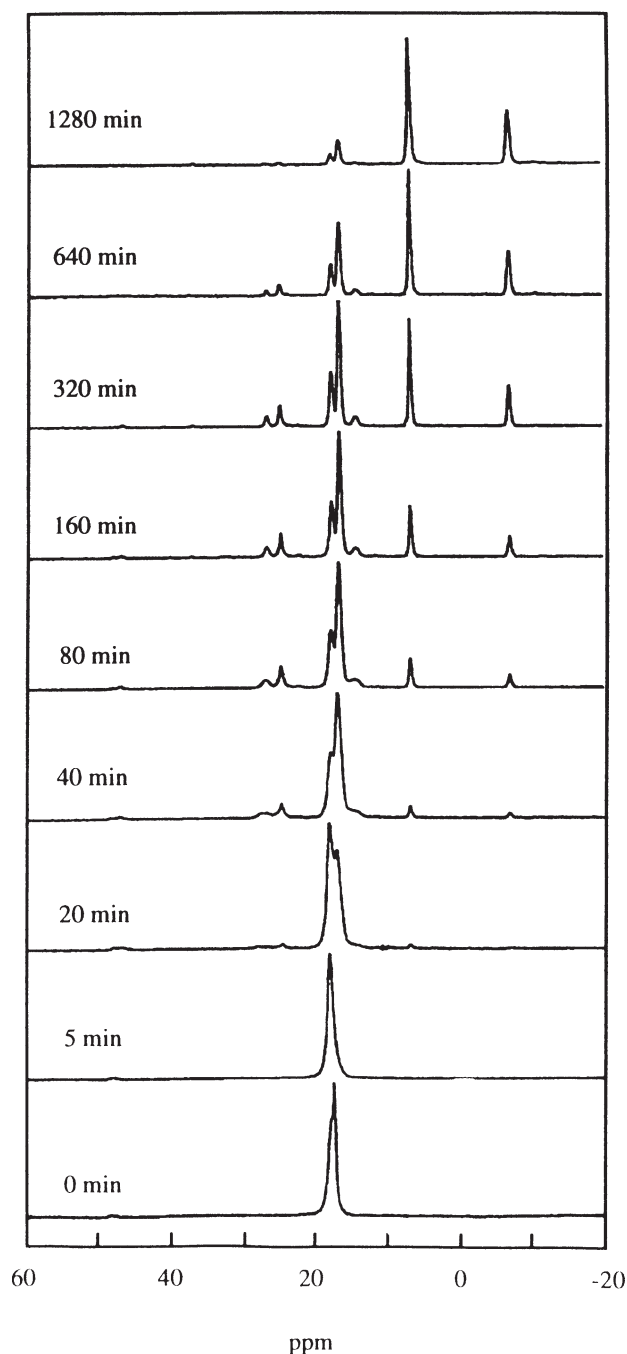


Figure 6. ^{13}C MAS NMR spectra observed after reaction of propane-2- ^{13}C (4 molecules/u.c.) at 573 K on H-ZSM-5 (Si/Al = 35).

belled methylene group of propane-2- ^{13}C . After 5 min at 573 K, a resonance is observed at ca. 16 ppm corresponding to the methyl group of propane. This assignment was confirmed by acquiring the spectrum without proton decoupling. It showed that this line indeed splits into a quadruplet. No other resonances were observed in the spectrum at this stage, indicating the absence of other products. Complete scrambling of the ^{13}C label, leading to the expected 2:1 ratio of the methyl and methylene resonances, is observed after ca. 20 min. As scrambling of the ^{13}C label in propane can occur without the formation of other prod-

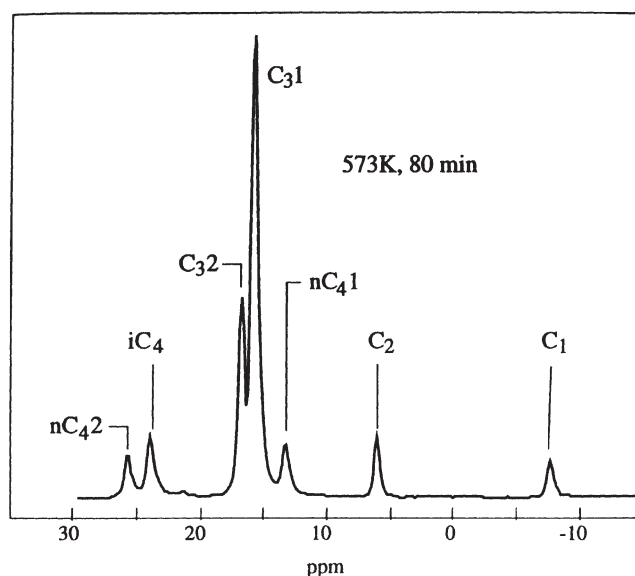


Figure 7. Detailed ^{13}C MAS NMR spectrum observed after reaction of propane-2- ^{13}C (4 molecules/u.c.) on Ga/H-ZSM-5 (Si/Al = 35) at 573 K for 80 min.

ucts, an observation which we have checked carefully, it can only occur via a cyclic intermediate.

Extremely low activity is observed for Ga/silicalite (Si/Al = 480), as shown in figure 5, compared to Ga/H-ZSM-5. Scrambling only occurs at ca. 723 K. It demonstrates that Brønsted acidity is necessary to activate propane at 573 K on Ga/H-ZSM-5 catalysts. Lower activity is also observed for H-ZSM-5 (figure 6). Scrambling is only detected after 20 min at 573 K and completed after ca. 80 min. Thus, Ga sites and Brønsted acid sites act in synergy. It is further noticed that identical spectra are observed for the Ga/H-ZSM-5 and H-ZSM-5 catalysts at longer reaction times (figures 4 and 6), from which we conclude that the major role of the Ga species in Ga/H-ZSM-5 is to promote the initial activation of propane.

Figure 7 details the spectrum observed after reaction of propane-2- ^{13}C on Ga/H-ZSM-5 for 80 min at 573 K. Besides scrambling of the ^{13}C label in propane, the reaction products are methane, ethane, *n*-butane, and *i*-butane. Figure 4 shows that those are formed once scrambling has taken place.

It was further demonstrated that dihydrogen inhibits the activation of propane (figure 8). This effect may be due to competitive adsorption of H_2 on the Ga species or even to reduction of Ga^{3+} to Ga^+ . The reduction of Ga_2O_3 to Ga_2O in such conditions has been reported [65–67].

All these observations can be accounted for by a bifunctional reaction step (BREST) mechanism (figure 9) [26]. The active site responsible for the activation of propane consists of a $(\text{Ga}^{3+}, \text{O}^{2-})$ ion pair closely associated with an acidic Brønsted site of the zeolite. The $(\text{Ga}^{3+}, \text{O}^{2-})$ ion pair involves either ion-exchanged gallium (Ga_{ionex}) and an oxygen anion from the zeolite lattice, or dispersed extra-framework Ga species (Ga_{d}) which may contain oxygen if they are (hydroxy) cations or neutral species, or are as-

sociated to zeolite oxygen anions otherwise. We propose that propane interacts heterolytically with the ($\text{Ga}^{3+}, \text{O}^{2-}$) ion pair via a positively and a negatively charged hydrogen atom, respectively, and that it is further converted into a pseudo-cyclopropane entity which is protonated by the Brønsted site. This scheme agrees with the heterolytic activation/dissociation of propane as ($\text{C}_3\text{H}_7^+, \text{H}^-$) on an oxidic Ga component which was proposed previously [68,69]. However, the role of Ga sites only was claimed in these reports and the existence of a cyclic intermediate was not identified. Upon chemisorption of propane, Ga^{3+} in the active site is formally reduced to Ga^+ and Ga is present as dispersed Ga hydride. This model is consistent with recent Ga K-edge EXAFS data [67] claiming that active Ga species in Ga/H-ZSM-5 are highly dispersed, probably as Ga hydride coordinated to basic oxygens in the zeolite channels.

The BREST scheme explains the ^{13}C scrambling in propane without formation of other products and the synergistic action of Ga species and Brønsted sites. The protonated pseudo-cyclopropane (PPCP) intermediate can evolve in different ways, as shown in figure 10.

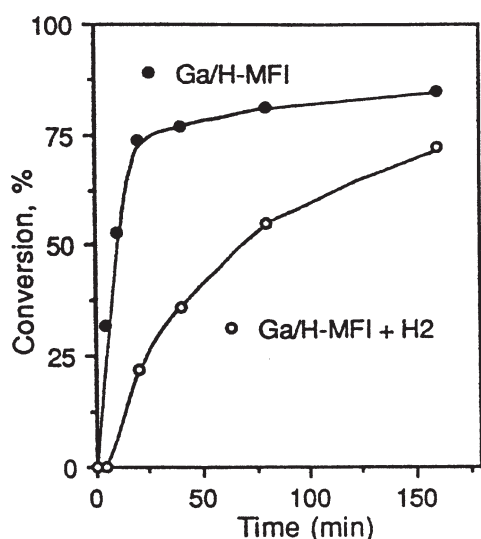


Figure 8. Effect of hydrogen on propane-2- ^{13}C conversion over Ga/H-ZSM-5 (Si/Al = 35) at 573 K.

1. It can yield a C_3H_9^+ carbocation bound to the zeolite framework. Deprotonation of this propenium ion recovers the zeolite acid site and propane, explaining the scrambling of the ^{13}C label in propane.
2. A C_3H_7^+ carbenium ion bound to the zeolite framework and dihydrogen are obtained if ruptures occur along 1. The C_3H_7^+ carbenium ion may further decompose into propene or oligomerize and restore the original zeolite Brønsted site.
3. Methane and a C_2H_5^+ carbenium ion bound to the zeolite framework are formed if ruptures occur along 2. C_2H_5^+ may restore the Brønsted acid site if it decomposes to ethene or oligomerizes. This mechanism as well as the above could account for non-observed species, supposed to be olefinic oligomers as their resonances are broadened beyond the detection limit, and explain the observation of small amounts of methane as a primary reaction product, even at very low conversion [23,52].
4. The PPCP intermediate can also decompose into ethane and a CH_3^+ carbocation bound to the zeolite framework if rupture occurs along 3. This CH_3^+ carbocation can react further with olefins and alkanes. The reaction of CH_3^+ (stabilized on a basic zeolite oxygen anion) with propane (activated on the Ga site) may yield *n*-butane or *i*-butane. These products are indeed observed in the initial reaction stages.

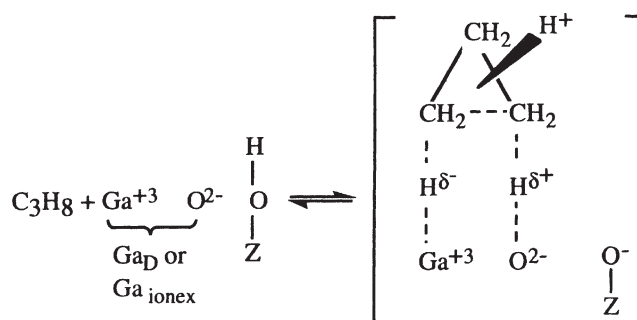


Figure 9. Bifunctional reaction step (BREST) mechanism for the bifunctional activation of propane on Ga-containing H-ZSM-5 catalyst: the protonated pseudo-cyclopropane (PPCP) intermediate.

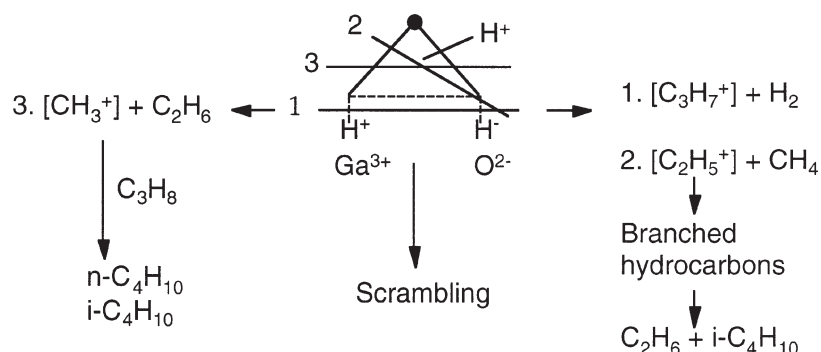


Figure 10. Initial products and intermediates resulting from the bifunctional activation of propane on Ga-containing H-ZSM-5 catalysts.

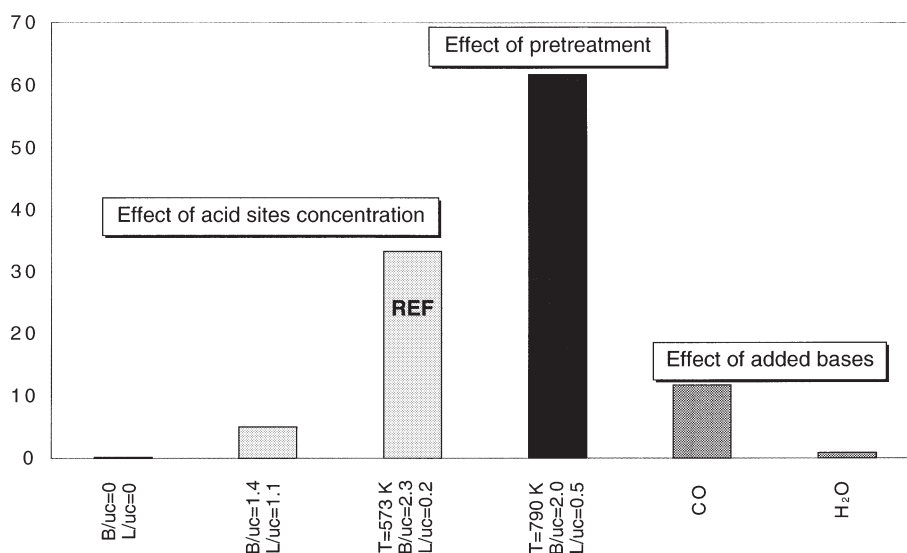


Figure 11. Variation of the initial rates (arbitrary units) of ^{13}C label scrambling in propane with protonic and aprotic sites contents, conditions of catalyst pretreatment, and addition of weak bases (samples: see table 3).

The PPCP intermediate model and the BREST reaction scheme agree well with the observed activation of propane by dissociative adsorption on Ga species [68–70], the proposed role of Ga species as hydrogen “portholes” [71], and the negative reaction order with respect to dihydrogen when extra-framework Ga species are present [70]. It also rationalizes several earlier mechanistic proposals claiming either the propane activation by acidic sites only [53,72] and the dehydrogenation of propane on Ga species [52,68,73].

^{13}C scrambling was also observed in the early stage of propane activation over H-ZSM-5 catalysts (figure 6) [25,28]. The BREST mechanism cannot be extended to pure H-ZSM-5 catalysts as no dehydrogenation sites are available. In the absence of a dehydrogenation function, ^{13}C scrambling in propane may however occur via a cationic transition state, i.e., C-ethanemethonium (C_3H_9^+), cycloproponium (C_3H_7^+), or a long chain carbenium ion. Such transition states were proposed by Olah [75] to rationalize hydrocarbon reactions in superacidic media.

The formation of C-ethanemethonium can occur by protolytic attack on C–H or C–C bonds, yielding initially H-proponium or C-proponium pentacoordinated ions, respectively. Proponium ions may further rearrange to the isomeric C-ethanemethonium ion. The exact nature of the initial interaction between a proton and propane is of little importance since rearrangements of energetically close carbonium ion forms take place easily [75].

^{13}C scrambling via a cycloproponium transition state requires the primary formation of a 2-propenium ion, followed by its rearrangement to 1-propenium and eventually cycloproponium ions. The formation of long chain carbenium ions also requires the primary formation of the 2-propenium ion, followed in this case by oligomerization and cracking.

The C-ethanemethonium mechanistic pathway involves Brønsted sites, while the two mechanisms implying a

2-propenium ion need Lewis acid sites for H^- abstraction when the reaction occurs in the absence of olefins. Hence, distinguishing between the roles of Brønsted and Lewis acid sites is necessary to elucidate the mechanism responsible for the activation of propane on the H-form of zeolites. Catalysts with different concentrations of protonic and aprotic acid sites (table 4) were used for this purpose and the effect of the addition of weak bases was investigated (experiments 5 and 6 in table 3). The results are shown in figure 11.

No correlation was observed between catalytic activity and the concentration of Lewis acid sites. In contrast, the concentration and the strength of the Brønsted acid sites govern the activity of all catalysts. Pretreating H-ZSM-5(35) at 790 K for 48 h (pretreatment B) doubles the amount of Lewis acid sites and slightly reduces (10%) the amount of Brønsted acid sites, relative to H-ZSM-5(35) activated at 573 K for 8 h (pretreatment A), as shown in table 4. Pretreatment B increases the conversion of propane-2- ^{13}C by a factor of about 2. This drastic increase of the reaction rate after pretreatment at high temperature is attributed to the generation of hyperactive sites (enhanced activity sites), which can be formed after removal of residual Na^+ or NH_4^+ [59,76,77] or under certain steaming conditions [78–80]. The addition of weak bases which poison acidic sites, leads to a substantial decrease of the scrambling rate, the stronger the base the more drastic its effect. Under otherwise identical conditions, initial scrambling rates decrease by a factor of 3 in the presence of CO and by at least an order of magnitude in the presence of H_2O .

The correlation observed between the initial rate of propane scrambling and the number and strength of the Brønsted sites, and the inhibiting effect of co-adsorbed weak bases observed using pure H-ZSM-5 catalysts suggest that strong protonic sites are responsible for the activation of propane and that aprotic sites do not play a direct role.

Aprotic (Lewis) sites can, however, have an indirect role when they enhance the acid strength of nearby Brønsted sites, as mentioned above.

We investigated also the effect of small amounts of propene on the activation of propane. In the presence of propene (experiment 7 in table 3), the temperature at which propane activation is firstly observed is 50 K lower than with propane alone. Along with ^{13}C scrambling in propane, *i*-butane is the main reaction product in the very early stage of the reaction.

The formation of *i*-butane is consistent with a classical carbenium ion mechanism [74,76,81,82]. Indeed, carbenium ions formed from non-labelled propene oligomers can abstract a hydride ion from labelled propane and the labelled propenium-2 ion can further react with non-labelled propene oligomers, transferring firstly the label to the oligomers and subsequently to their cracking products, i.e., *i*-butane and propane. This mechanism justifies the formation of labelled *i*-butane as a primary product of the conversion of propane-2- ^{13}C in the presence of propene. It also accounts for the formation of propane-1- ^{13}C and, therefore, the scrambling of the ^{13}C label in propane.

In conclusion, propane is activated on Brønsted sites. The activity of the Brønsted sites is increased by either the presence of Ga species (bifunctional catalysis) or Lewis acid sites (enhanced strength). In Ga/H-ZSM-5 catalysts, propane activation occurs at low temperature via the cyclic PPCP intermediate. Other carbenium routes become more important in the absence of Ga (higher *i*-C₄ yield) or in the presence of olefins (propene).

3.3. ^{13}C in situ MAS NMR investigation of the alkylation of benzene with propane

The alkylation of benzene with alkanes has been reported to occur in superacidic media [83,84]. Two competitive mechanisms were suggested to account for cumene formation from benzene and propane [84]. However, these mechanisms cannot readily be extended to the benzene alkylation of propane using zeolite catalysts as different reaction products are observed [85–87]. ^{13}C in situ MAS NMR was used to clarify the mechanism of the benzene alkylation with propane using Ga/H-ZSM-5 catalysts [27].

When benzene is adsorbed in the presence of hydrogen (experiment A in table 5), the NMR resonance of adsorbed benzene is shifted significantly to higher field relative to solution data, indicating some distortion of benzene upon adsorption.

Co-adsorption of propane (experiments C and D in table 5) results in a shift of benzene resonance to lower field. The presence of benzene, in turn, affects the resonance corresponding to the labelled methylene group of propane appearing now as a narrow and a broad line, both centered at ca. 17 ppm. The narrow line, identical to the resonance observed when propane alone is adsorbed (experiment B in table 5), is attributed to propane molecules which have a certain degree of mobility. The broad line corresponds to

propane molecules with restricted mobility as evidenced by cross-polarization experiments. Restricted propane mobility in the presence of benzene may be due to the decreased space available within zeolite channels following benzene adsorption or, more likely, to a specific interaction of the propane methylene group with adsorbed benzene.

Indeed, 9 molecules of benzene per zeolite unit cell are sufficient to affect all the acidic and Ga sites of the catalyst, benzene being either H-bonded to the surface acidic OH groups and/or electron-bonded to the Ga sites. Hence, some positive charge can be transferred to the benzene molecule, resulting in the formation of a weak acid. The latter can interact with propane, considered to be a weak base, and thereby disturb the methylene group resonance.

The reaction of propane with benzene begins at 573 K, as also observed when propane only is adsorbed. However, a long induction period (40–160 min) whose duration increases with the benzene/propane ratio is observed. During this induction period, the broad resonance line at ca. 17 ppm, corresponding to propane molecules with restricted mobility shifts to lower field and becomes more pronounced. It then disappears when the first reaction products are formed. It suggests that the stronger adsorption of benzene relative to propane and/or the interaction between adsorbed benzene and the propane methylene group prevent the direct activation of propane on the zeolite active sites, leading to an induction period, and that the propane molecules with restricted mobility are those reacting initially with benzene.

Benzene alkylation with propane can be initiated in two different ways (figure 12) [76]:

1. Benzene activation by H-ZSM-5 was reported to occur by benzene protonation on strong acid sites to form a benzenium ion [88]. The benzenium ion can abstract a hydride ion from the nearest propane molecule leading to an isopropenium ion. The latter can alkylate benzene to yield cumene which in turn can convert to toluene and ethylbenzene via secondary reactions [21,89].
2. Propane activation by Ga/H-ZSM-5 occurs via a bifunctional mechanism involving the cyclic PPCP intermediate. The latter can decompose in various ways resulting in the formation of CH₄, C₂H₆, H₂ and methyl, ethyl and propyl carbenium ions (figure 10). These carbenium ions can lead to the corresponding alkylbenzene: toluene, ethylbenzene, cumene and *n*-propylbenzene when the reaction is carried out in the presence of benzene.

^{13}C in situ MAS NMR results indicate that both activation pathways probably operate under our reaction conditions.

The appearance of the small but distinct NMR line at ca. 124.4 ppm in the very early stage of the reaction, which disappears at longer reaction times, shows the formation of cyclohexadienes. Weak resonances at ca. 23.5 and 34 ppm also evidence the formation of small amounts of cumene

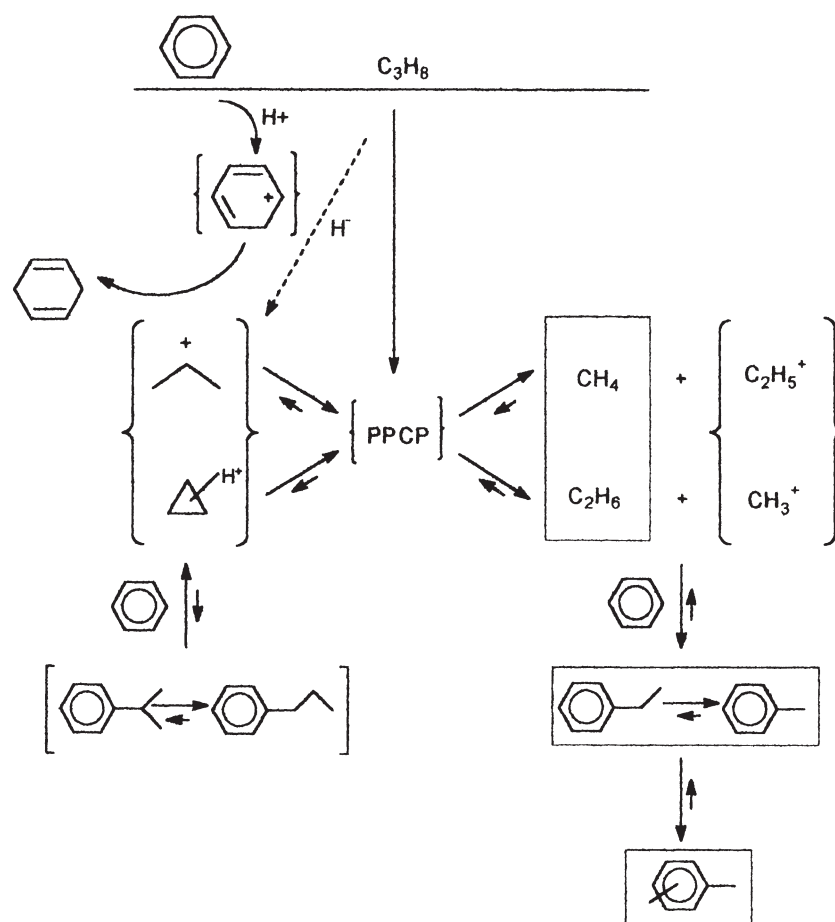


Figure 12. Proposed mechanism for the benzene alkylation with propane over Ga/H-ZSM-5 catalyst.

labelled in the α and β positions of the alkyl chain, respectively. These observations favor the first activation pathway.

The progressive shift of the methylene resonance line at 17 ppm to higher field, as reaction initially proceeds, indicates that the resonance corresponding to the propane methyl group may appear at ca. 16 ppm. The resonances of the methylene and methyl groups of propane are not well resolved in the presence of benzene because of significant line broadening. The scrambling of the ^{13}C label in propane implies a PPCP-type intermediate and points to the second activation pathway.

Although evidence for both routes exists, the observation of an induction period suggests that the activation pathway involving the preliminary activation of propane is dominant.

In the initial stages of the reaction (experiments C and D in table 5), major resonances corresponding to toluene (21 ppm), ethylbenzene (29 ppm), ethane (7 ppm), and methane (−6 and −11 ppm) are observed together with weak resonances attributed to cyclohexadienes (124.4 ppm), cumene (23.5 and 34 ppm) and *n*-propylbenzene (14 and 25 ppm). After heating for 300 min at 573 K, the lines corresponding to cyclohexadiene and cumene disappear, and toluene and methane become the major reaction products. Longer reaction times cause ethylbenzene and *n*-propylbenzene to disappear, while the amounts of

toluene, xylenes, ethane and methane increase. Eventually, toluene and xylenes are converted into condensed aromatics. These observations support the general scheme shown in figure 12.

It should, however, be noted that acidic zeolite catalysts can also convert cumene and *n*-propylbenzene to toluene and ethylbenzene by cracking of their alkyl chain [21,24,89]. In order to check if toluene and ethylbenzene are the products of direct alkylation or a consequence of cumene and *n*-propylbenzene cracking, the reaction of cumene- α - ^{13}C was carried out in the presence of benzene under similar reaction conditions (experiment E in table 5).

Cumene is predominantly converted to *n*-propylbenzene and small amounts of toluene and ethylbenzene after only 1 min at 573 K. Further heating at 573 K causes the disappearance of the lines corresponding to cumene and *n*-propylbenzene while a resonance at 16 ppm grows simultaneously. The latter corresponds to the methyl or methylene groups of propane. Thus, the conversions of cumene and *n*-propylbenzene at 573 K occur via dealkylation. Propene is not observed due to its rapid self-hydrogenation or oligomerization in our batch conditions [9,22,23]. Propane, activated via a PPCP-type mechanism can react further with benzene or other alkylaromatics to yield various methyl-substituted aromatic compounds (e.g., toluene and xylenes). This is confirmed by disappearance of

the propane resonance at ca. 16 ppm and the appearance of the resonance centered at ca. 20 ppm already observed for the alkylation of benzene with propane. These observations indicate that the formation of methyl-substituted aromatics from cumene and *n*-propylbenzene requires propane as an intermediate.

The overall reaction scheme is shown in figure 12. The following conclusions are drawn:

1. When benzene and propane are co-adsorbed on Ga/H-ZSM-5, benzene is preferentially adsorbed on the acidic and Ga sites of the zeolite, and two types of propane species co-exist, characterized by different mobilities.
2. The induction period for the alkylation of benzene with propane results from the stronger adsorption of benzene and the interaction of adsorbed benzene with the methylene group of propane, preventing the direct activation of propane via the BREST mechanism and the PPCP intermediate.
3. The dominant reaction mechanism includes the formation of the PPCP intermediate, its evolution towards CH_3^+ , C_2H_5^+ and C_3H_7^+ carbenium ions, and their subsequent reaction with benzene to give toluene, ethylbenzene, cumene and *n*-propylbenzene, respectively. The alkylation products are mainly toluene, xylenes, and ethylbenzene. The alkyl chains of cumene and *n*-propylbenzene eventually undergo cracking at 573 K.

3.4. Structural study of VPI-5

VPI-5 is an aluminophosphate, AlPO_4 , molecular sieve with 18-membered ring unidimensional channels [90,91]. On the basis of simulated powder XRD patterns, Rudolf and Crowder [92] refined the structure of the fully hydrated VPI-5 to the $\text{P6}_3\text{cm}$ space group. Later, McCusker et al. [93] concluded to a lower P6_3 space group (figure 13 (a) and (b)).

The former structure contains two Al and P crystallographic sites and only 4-coordinated Al atoms. It is difficult to reconcile with the ^{27}Al and ^{31}P MAS NMR spectra [91,94] as the ^{31}P spectrum of VPI-5 shows three resonances with intensity ratio 1:1:1 and the ^{27}Al spectrum evidences resonances characteristic of 4- and 6-coordinated Al with intensity ratio 2:1. In contrast, the latter structure is consistent with the ^{27}Al and ^{31}P MAS NMR spectra as there are three distinct P and Al crystallographic sites. The second structure refinement also locates the water molecules inside the VPI-5 pores: two molecules (referred to as “framework” water) link the Al atoms between the fused 4-membered rings, thus making one-third of Al atoms 6-coordinated; the remaining water molecules (referred to as “free” water) form a triple helix. ^{27}Al and ^{31}P MAS NMR investigations which are more sensitive to local ordering than XRD resolve this controversy.

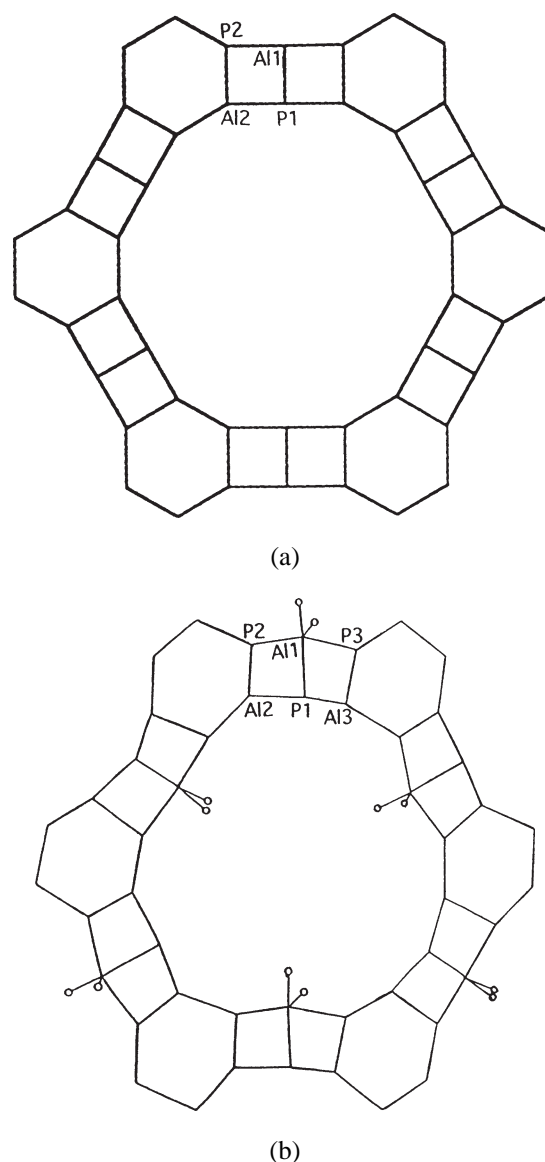


Figure 13. One layer of the VPI-5 framework (AFI) structure along the [001] direction according to Rudolf et al. [92], showing $\text{P6}_3\text{cm}$ symmetry (a), and according to McCusker et al. [93], showing the P6_3 symmetry (b). Intracrystalline water is not shown, except for the “framework” water.

^{31}P MAS NMR spectra of fully hydrated VPI-5 in the range 294–353 K are shown in figure 14(a). At 294 K, the ^{31}P NMR spectrum shows three resonances with intensity ratio 1:1:1 corresponding to three crystallographic sites in the VPI-5 structure. In agreement with the results reported by Houckgeest et al. [95], changes in the NMR spectrum are already observed at 338 K and they become prominent at 343 K. The resonance at -27 ppm grows at the expense of that at -23 ppm. The two resonances do not coalesce and the growing peak only shifts slightly from -27.3 ppm at 294 K to -26.7 ppm at 348 K while the resonance decreasing in intensity shifts gradually from -23.4 to ca. -25 ppm. The transformation is complete at 353 K and the final spectral intensity ratio is 2:1, indicating that the VPI-5 structure contains only two crystallographic sites

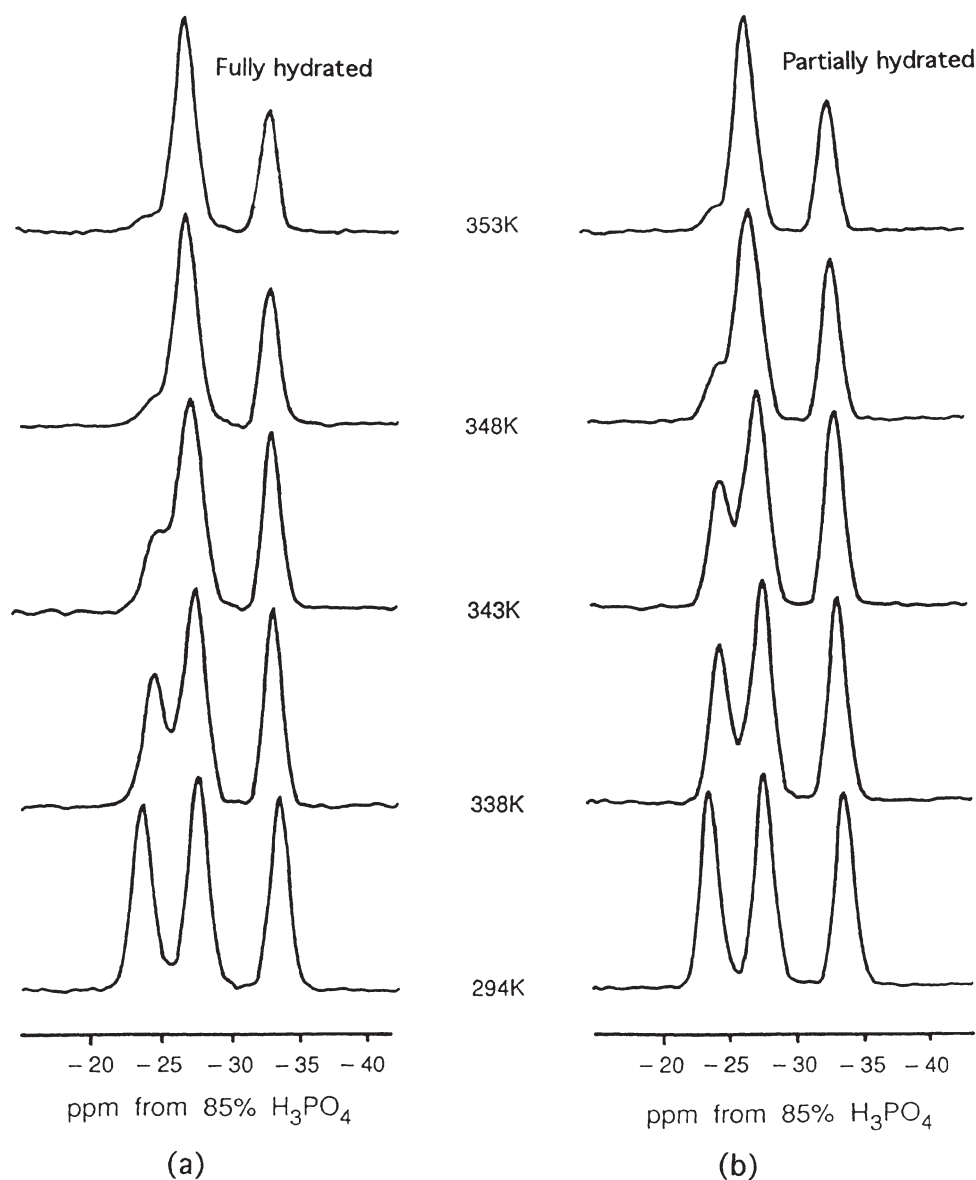


Figure 14. Variable-temperature ^{31}P MAS NMR spectra of fully hydrated VPI-5 (a) and partially hydrated VPI-5 (b).

at 353 K with a population ratio of 2:1. The transformation is fully reversible. A considerable decrease of the intensity of ^1H - ^{31}P CP/MAS lines is also observed when temperature is increased from 294 to 330 K. These NMR results agree with other reports [96–100].

The ^{27}Al MAS NMR spectrum of fully hydrated VPI-5 at 294 K (figure 15(a)) shows 4- and 6-coordinated Al resonances in the 2:1 intensity ratio, centered at 40 and -18 ppm, respectively. The intensity ratio of 4-coordinated/6-coordinated Al remains constant, ca. 2:1, in the temperature range 294–370 K. The shape and linewidth of the resonance at 40 ppm do not change significantly. In contrast, the second-order quadrupolar powder pattern of the resonance at -18 ppm varies with temperature and simulations of this pattern yield the quadrupolar coupling constant, C_Q , the asymmetry parameter, η , and the isotropic chemical shift, δ (figure 15(b)). In agreement with the ^{31}P results, a considerable decrease in the intensity of the

^1H - ^{27}Al CP/MAS line is observed when the temperature is increased from 294 to 330 K.

^{27}Al MAS nutation spectra in the 4-coordinated Al region of the spectrum, ca. 40 ppm (figure 16) provide further insight into the structural change. At 294 K, the spectrum shows one line at $\omega_{\text{rf}}/2\pi$ and two lines between $\omega_{\text{rf}}/2\pi$ and ca. $3\omega_{\text{rf}}/2\pi$. It shows that the two 4-coordinated Al lines which overlap in the normal MAS NMR mode are characterized by different quadrupolar interaction parameters. When temperature is increased to 343 K, the resolution of the two peaks from 4-coordinated Al decreases considerably and only one line is detected at 370 K. In agreement with the ^{31}P NMR results, it suggests that above 343 K the two 4-coordinated Al sites become equivalent.

In addition, the linewidth of the ^1H MAS NMR line of water in fully hydrated VPI-5 narrows from 1220 Hz at 294 K to 300 Hz at 353 K, implying that mobility of water

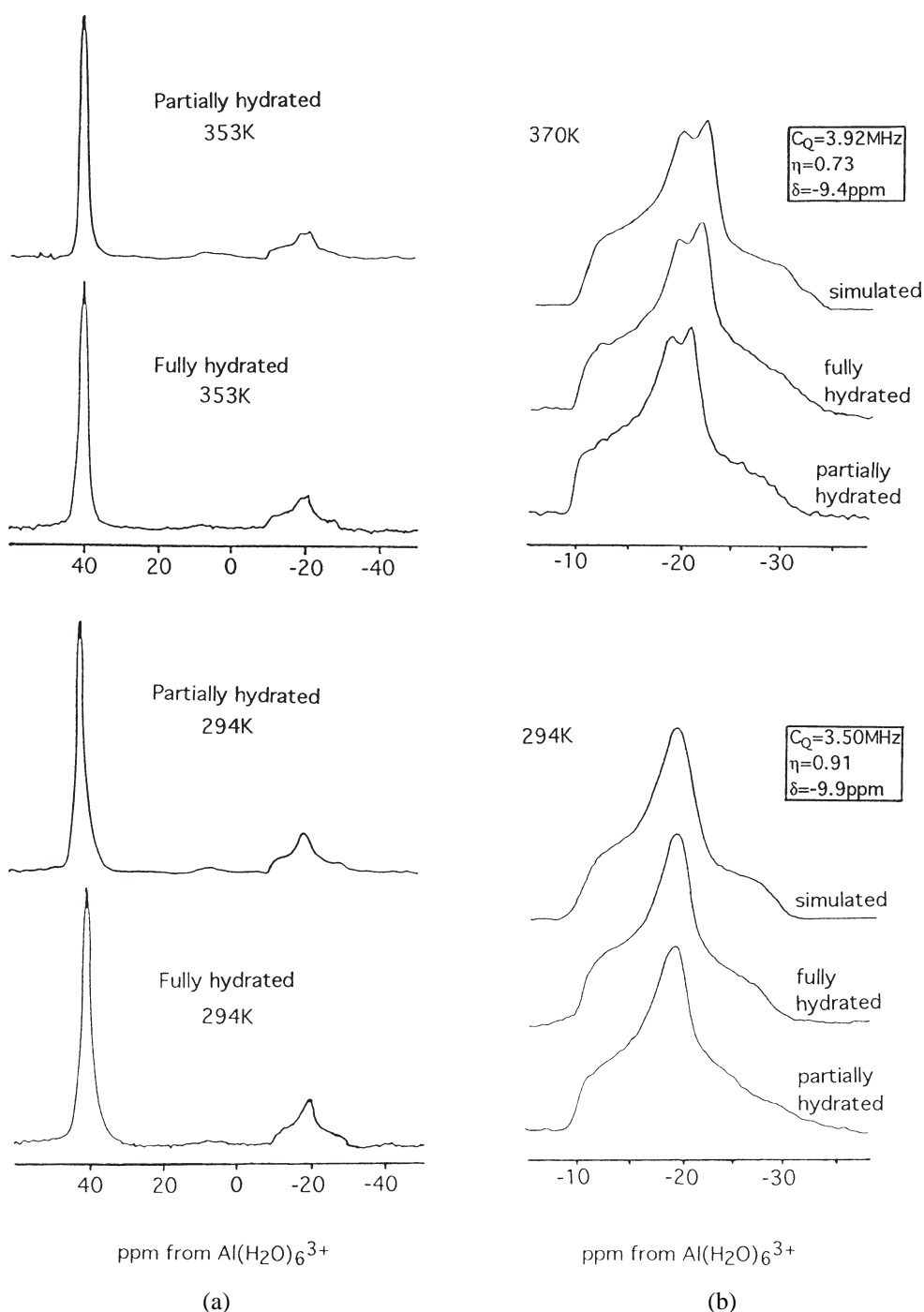


Figure 15. ^{27}Al MAS NMR spectra measured at 294 and 353 K of fully and partially hydrated VPI-5 (a), and comparison of the experimental and simulated 6-coordinated Al second-order quadrupolar line shapes of fully and partially hydrated VPI-5 at 294 and 370 K (b).

increases, i.e., that the triple helix of water molecules is less ordered as temperature increases.

The MAS NMR spectra of VPI-5 in the temperature range 294–370 K show that VPI-5 undergoes a symmetrical change from the $P6_3$ space group at ambient temperature to $P6_3\text{cm}$ above 353 K. However, the cause of this structural change was not clear at that time. Houckgeest et al. [95] proposed that the symmetry change from the $P6_3$ space group to the $P6_3\text{cm}$ space group, in fully hydrated VPI-5, results from the breakdown of the triple-helix struc-

ture of water inside VPI-5 channels. It implies that VPI-5 without free water molecules should have the $P6_3\text{cm}$ space group at room temperature. CA MAS NMR was used to test this hypothesis, namely by studying partially hydrated VPI-5 materials.

The preparation of partially hydrated VPI-5, containing only “framework” water, can be monitored by ^2H NMR and by ^{27}Al and ^{31}P MAS NMR. Figure 17(a) shows that the ^2H NMR spectrum of fully hydrated (10% D_2O + 90% H_2O) VPI-5 heated to 373 K in a sealed rotor has a nar-

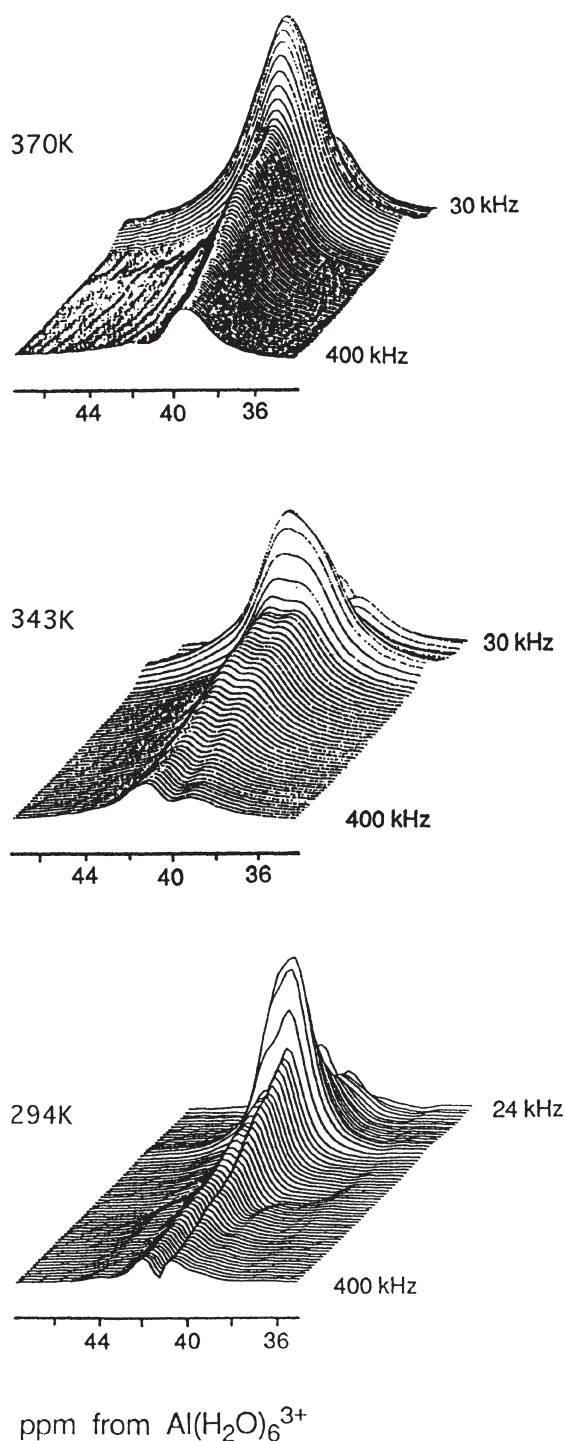


Figure 16. Variable-temperature ^{27}Al MAS nutation spectra in the region of 4-coordinated Al of fully hydrated VPI-5 measured with a $\omega_{\text{rf}}/2\pi = 115 \pm 5$ kHz radiofrequency field.

row central peak and a characteristic spin-1 powder pattern. Goldfarb et al. [101] concluded that the narrow line probably comes from D_2O adsorbed on the VPI-5 crystal surface. After heating to 373 K for 15 min in an open-cap rotor (until there is no further change of lineshape), only the powder pattern remains (figure 17(b)). The ^2H NMR simulations suggest that the latter arises from the rotation of two “framework” water molecules around their C_2 -axes,

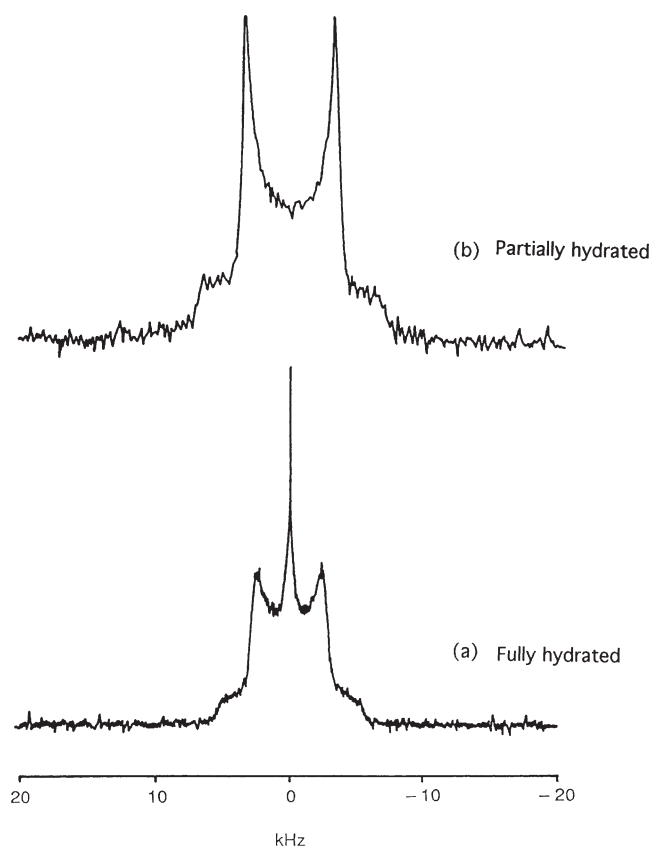


Figure 17. ^2H NMR spectra measured at 373 K of fully hydrated (a) and partially hydrated VPI-5 (b).

although at higher water contents the “free” water molecules may also contribute. Thus, the sample prepared as above and characterized by the ^2H NMR spectrum shown in figure 17(b) contains only “framework” water. This fact was further confirmed by ^{27}Al and ^{31}P MAS NMR.

The ^{31}P MAS NMR spectra (figure 14(b)) show that both fully and partially hydrated VPI-5 undergo the same structural change between 294 and 353 K. The ^{31}P chemical shifts are almost identical for both samples. A closer look at the intensity ratio of the resonances at -23 and -27 ppm suggests that the temperature at which structural symmetry change for partially hydrated VPI-5 is slightly higher than for fully hydrated VPI-5. Perez et al. [102] who measured ^{31}P MAS NMR spectra of VPI-5 with different water contents found that the spectrum of a partially hydrated sample, such as that described here or dehydrated further, has an additional low intensity resonance at -30.8 ppm. We did not find this to be the case, even for extensively dehydrated samples (figure 14(b)).

Figure 15(a) shows that both fully and partially hydrated VPI-5 have nearly identical ^{27}Al MAS NMR spectra at different temperatures, which means that only the “free” water was removed. However, a small increase of the linewidth of the 4-coordinated Al resonance is observed for the partially hydrated sample as temperature is increased, indicating that the environment of the 4-coordinated Al atoms may be altered when “free” water molecules are removed.

In conclusion, MAS ^{27}Al , ^{31}P , and ^{27}Al nutation NMR spectra prove that VPI-5 has three crystallographic sites at 294 K, thus confirming the XRD structure of fully hydrated VPI-5 proposed by McCusker et al. [93]. Both fully and partially hydrated VPI-5 undergo identical and reversible symmetry changes at similar temperature, from the P6_3 space group at ambient temperature to the $\text{P6}_3\text{cm}$ space group above 353 K. The environment of the 6-coordinated Al atoms in partially hydrated VPI-5 is not affected by “free” water molecules since the quadrupolar parameters and isotropic chemical shifts are similar to those observed at the same temperature for the fully hydrated sample. The environment of the 4-coordinated Al atoms, however, changes slightly. Thus, the symmetry change does not involve “free” water molecules but either the “framework” water molecules and/or specific properties of the VPI-5 framework itself.

4. Conclusion

In situ MAS NMR, combined with the strategic ^{13}C labelling of organic reactants, is a powerful technique for the detailed investigation of catalytic transformations. The main advantages of *in situ* MAS NMR relative to other spectroscopies which could also provide molecular and mechanistic information are the ease with which it can identify species present in the NMR cell and the possibility to fully quantitate those. It may, in this respect, have some advantage over fully *in situ* MAS NMR which is currently being developed.

We have shown in this review, using some examples from our own work, that *in situ* MAS NMR can unveil the mechanistic detail of complex reactions by carefully designing experiments and provide insight into the nature and evolution of surface species. *In situ* MAS NMR can also be used to obtain information about structural catalyst modifications.

While *in situ* MAS NMR can undoubtedly identify the intermediates and products of a catalytic transformation, using their ^{13}C -labelled carbon atom chemical shifts as fingerprints, its rational application to mechanistic studies and the derivation of a reaction mechanism require a close interaction of the NMR expert with organic and catalytic chemists possessing a broad view and a good understanding of reaction mechanisms.

MAS NMR is also a powerful method for the characterization of catalyst structure. It can detect small structural changes resulting from slight modifications of the local ordering. This information is not easily accessible by powder X-ray diffraction.

Acknowledgement

The work reported here has greatly benefitted from the contributions of colleagues at the Facultés Universitaires de Namur, Cambridge University, and Moscow University. It

has been supported financially by several industrial companies and institutions: Haldor Topsøe A/S, Petronas, Rhône Poulenc, and the Belgian National Research Foundation (FNRS). All of them are hereby acknowledged for their collaboration and support.

References

- [1] G. Engelhardt and D. Michel, in: *High-Resolution Solid-State NMR of Silicates and Zeolites* (Wiley, New York, 1987).
- [2] J. Klinowski, *Chem. Rev.* 91 (1991) 1459.
- [3] A.T. Bell and A. Pines, *NMR Techniques in Catalysis* (Dekker, New York, 1994).
- [4] J.F. Haw, in: *NMR Techniques in Catalysis* (Dekker, New York, 1994) p. 139, and references therein.
- [5] I.I. Ivanova and E.G. Derouane, *Stud. Surf. Sci. Catal.* 85 (1994) 357, and references therein.
- [6] T.A. Carpenter, J. Klinowski, D.T.B. Tennakoon, C.J. Smith and D.C. Edwards, *J. Magn. Reson.* 68 (1986) 561.
- [7] E.J. Munson, D.B. Ferguson, A.A. Kheir and J.F. Haw, *J. Catal.* 136 (1992) 504.
- [8] J.F. Haw, *Spec. Publ. Roy. Soc. Chem.* 114 (1992) 1.
- [9] J.F. Haw, B.R. Richardson, I.S. Oshiro, N.D. Lazo and J.A. Speed, *J. Am. Chem. Soc.* 111 (1989) 2052.
- [10] E.J. Munson, D.K. Murray and J.F. Haw, *J. Catal.* 141 (1993) 733.
- [11] H. Ernst, D. Freude and T. Mildner, *Chem. Phys. Lett.* 229 (1994) 291.
- [12] H. Ernst, D. Freude, T. Mildner and I. Wolf, *Solid State NMR* 6 (1996) 147.
- [13] T. Mildner, H. Ernst, D. Freude and W.F. Hoelderich, *J. Am. Chem. Soc.* 119 (1997) 4258.
- [14] G.W. Haddix, J.A. Reiner and A.T. Bell, *J. Catal.* 106 (1987) 111.
- [15] G.W. Haddix, J.A. Reiner and A.T. Bell, *J. Phys. Chem.* 93 (1989) 5859.
- [16] M. Hunger and T. Horvath, *J. Chem. Soc. Chem. Commun.* (1995) 1423.
- [17] M. Hunger and T. Horvath, *J. Catal.* 167 (1997) 187.
- [18] P. Goguen and J.F. Haw, *J. Catal.* 161 (1996) 870.
- [19] J.F. Haw, P.W. Goguen, T. Xu, T.W. Skloss, W. Song and Z. Wang, *Angew. Chem. Int. Ed. Engl.* 37 (1998) 948.
- [20] P.W. Goguen, T. Xu, D.H. Barich, T.W. Skloss, W. Song, Z. Wang, J.B. Nicholas and J.F. Haw, *J. Am. Chem. Soc.* 120 (1998) 2650.
- [21] I.I. Ivanova, D. Brunel, J.B. Nagy, G. Daelen and E.G. Derouane, *Stud. Surf. Sci. Catal.* 78 (1993) 587.
- [22] E.G. Derouane, S.B.A. Hamid, I.I. Ivanova, N. Blom and P.-E. Højlund-Nielsen, *J. Mol. Catal.* 86 (1994) 371.
- [23] I.I. Ivanova, N. Blom, S.B.A. Hamid and E.G. Derouane, *Rec. Trav. Chim. Pays-Bas* 113 (1994) 454.
- [24] I.I. Ivanova, D. Brunel, J.B. Nagy and E.G. Derouane, *J. Mol. Catal. A* 95 (1995) 243.
- [25] I.I. Ivanova, N. Blom and E.G. Derouane, *Stud. Surf. Sci. Catal.* 94 (1995) 419.
- [26] E.G. Derouane, S.B. Abd Hamid, A. Pasau-Claerbout, M. Seivert and I.I. Ivanova, *Stud. Surf. Sci. Catal.* 92 (1995) 123.
- [27] I.I. Ivanova, N. Blom and E.G. Derouane, *J. Mol. Catal. A* 109 (1996) 157.
- [28] I.I. Ivanova, E.B. Pomakhina, A.I. Rebrov and E.G. Derouane, *Topics Catal.* 6 (1998) 49.
- [29] I.I. Ivanova, A.I. Rebrov, E.B. Pomakhina and E.G. Derouane, *J. Mol. Catal.*, submitted.
- [30] H. He and J. Klinowski, *Catal. Today* 30 (1996) 119.
- [31] H. He, W. Kolodziejski and J. Klinowski, *Chem. Phys. Lett.* 200 (1992) 83.
- [32] H. He and J. Klinowski, *J. Phys. Chem.* 98 (1994) 1192.
- [33] G.A. Olah, ed., *Friedel-Crafts and Related Reactions*, Vol. 2 (Wiley, New York, 1964).

- [34] P.B. Venuto and P.S. Landis, *Adv. Catal.* 18 (1968) 259.
- [35] W.W. Kaeding and R.E. Holland, *J. Catal.* 109 (1988) 212.
- [36] I.I. Ivanova, I.A. Zen'kovich, T.A. Chemleva, K.V. Topchieva, N.F. Meged' and L.A. Lapkina, *Neftekhimija* 24 (1984) 805.
- [37] B.R. Richardson, N.D. Lazo, P.D. Schettler, J.L. White and J.F. Haw, *J. Am. Chem. Soc.* 112 (1990) 2886.
- [38] V.B. Kazansky and I.N. Senchenya, *Catal. Lett.* 8 (1991) 317.
- [39] C.D. Neitzescu, *Experimentia* 16 (1960) 332.
- [40] C.P. Neitzescu, I. Necsoiu, A. Geatz and M. Zolman, *Ber.* 92 (1959) 10.
- [41] J.E. Douglas and R.M. Roberts, *Chem. Ind.* (1959) 926.
- [42] D. Best and B.W. Wojciechowski, *J. Catal.* 47 (1977) 11.
- [43] H.K. Beyer and G. Borbely, in: *New Developments in Zeolite Science and Technology*, Proc. 7th Int. Zeolite Conf., eds. Y. Murakami, A. Iijima and J.W. Ward (Elsevier, New York, 1986) p. 867.
- [44] S. Fukase and B.W. Wojciechowski, *J. Catal.* 109 (1988) 180.
- [45] P.A. Jacobs, *Carboniogenic Activity of Zeolites* (Elsevier, New York, 1977).
- [46] M.L. Poutsma, *Am. Chem. Soc. Monogr.* 171 (1971) 431.
- [47] L. Random, J.A. Pople, V. Buss and P.V.R. Schleyer, *J. Am. Chem. Soc.* 93 (1971) 1813.
- [48] J. Sommer and J. Bukala, *Acc. Chem. Res.* 26 (1993) 370.
- [49] O.O. Parenago, O.E. Lebedeva, I.I. Ivanova, N.E. Vilyareal, L.E. Latysheva, S.A. Skornikova, V.V. Chenets and E.V. Lunina, *Kinet. Catal.* 34 (1993) 183.
- [50] P.A. Parikh, N. Subrahmanyam, Y.S. Bhat and A.B. Halgeri, *Appl. Catal.* 90 (1992) 1.
- [51] D. Fraenkel and M. Levy, *J. Catal.* 118 (1989) 10.
- [52] M. Guisnet, N.S. Gnep and F. Alario, *Appl. Catal.* 89 (1992) 1.
- [53] Y. Ono, *Catal. Rev. Sci. Eng.* 34 (1992) 179.
- [54] A. Brenner and P.H. Emmett, *J. Catal.* 75 (1982) 410.
- [55] W.O. Haag and R.M. Dessau, in: *Proc. 8th Int. Congress on Catalysis* (Verlag Chemie, Weinheim, 1984) p. 305.
- [56] H. Krannila, W.O. Haag and B.C. Gates, *J. Catal.* 135 (1992) 115.
- [57] J. Abbot, *J. Catal.* 126 (1990) 628.
- [58] J. Abbot, *Appl. Catal.* 57 (1990) 105.
- [59] J. Engelhardt and W.K. Hall, *J. Catal.* 125 (1990) 472.
- [60] G.M. Kramer, G.B. McVicker and J.J. Ziemiak, *J. Catal.* 92 (1985) 355.
- [61] G.B. McVicker, G.M. Kramer and J.J. Ziemiak, *J. Catal.* 83 (1983) 286.
- [62] R.A. Beyerlein, G.B. McVicker, L.N. Yacullo and J.J. Ziemiak, *J. Phys. Chem.* 92 (1988) 1967.
- [63] T. Mole, J.R. Anderson and G. Creer, *Appl. Catal.* 17 (1985) 141.
- [64] M.V. Vishnetskaya and B.V. Romanovskii, *J. Phys. Chem. (Rus.)* 67 (1993) 1740.
- [65] G.L. Price and V. Kanazirev, *J. Mol. Catal.* 66 (1991) 115.
- [66] G.L. Price and V. Kanazirev, *J. Catal.* 126 (1990) 267.
- [67] G.D. Meitzner, E. Iglesia, J.E. Baumgartner and E.S. Huang, *J. Catal.* 140 (1993) 209.
- [68] P. Meriaudeau, G. Sapaly and C. Naccache, *J. Mol. Catal.* 81 (1993) 293.
- [69] G. Buckles, G.J. Hutchings and C.D. Williams, *Catal. Lett.* 11 (1991) 89.
- [70] N.S. Gnep, J.Y. Doyemet, A.M. Seco, F. Ribeiro and M. Guisnet, *Appl. Catal.* 35 (1987) 93.
- [71] E. Iglesia, J.E. Baumgartner and G.L. Price, *J. Catal.* 134 (1992) 549.
- [72] M. Shibata, H. Kitagawa, Y. Sendoda and Y. Ono, in: *New Developments in Zeolite Science and Technology*, eds. Y. Murakami, A. Iijima and J.W. Ward (Kodansha-Elsevier, Tokyo, 1986) p. 717.
- [73] P. Meriaudeau and C. Naccache, *J. Mol. Catal.* 59 (1990) L31.
- [74] M. Daage and F. Fajula, *J. Catal.* 81 (1983) 394.
- [75] G.A. Olah, *J. Am. Chem. Soc.* 94 (1972) 808.
- [76] E.A. Lombardo, G.A. Sill and W.K. Hall, *J. Catal.* 119 (1989) 426.
- [77] P.O. Fritz and J.H. Lunsford, *J. Catal.* 118 (1989) 85.
- [78] R.M. Lago, W.O. Haag, R.J. Mikowsky, D.H. Olson, S.D. Hellring, K.D. Schmitt and G.T. Kerr, in: *Proc. 7th Int. Zeolite Conf.*, eds. Y. Murakami et al. (Kodansha, Tokyo, 1987) p. 677.
- [79] N.-Y. Töpsøe, F. Joensen and E.G. Derouane, *J. Catal.* 110 (1984) 404.
- [80] D.B. Lukyanov, *Zeolite* 11 (1991) 325.
- [81] F. Fajula, *Stud. Surf. Sci. Catal.* 20 (1985) 361.
- [82] J.L. White, N.D. Lazo, B.R. Richardson and J.F. Haw, *J. Catal.* 125 (1990) 260.
- [83] L. Schmerling and J.A. Vesely, *J. Org. Chem.* 38 (1973) 312.
- [84] G.A. Olah, P. Schiiling, J.S. Staral, Yu. Halpern and J.A. Olah, *J. Am. Chem. Soc.* 97 (1975) 6807.
- [85] T.V. Vasina, S.A. Isaev, O.V. Bragin and B.K. Nefedov, *US USSR No. 1426966* (1988).
- [86] O.V. Bragin, T.V. Vasina, S.A. Isaev and Kh.M. Minachev, *Izv. Akad. Nauk USSR Ser. Khim.* 7 (1987) 1682.
- [87] S.A. Isaev, T.V. Vasina and O.V. Bragin, *Izv. Akad. Nauk USSR Ser. Khim.* 10 (1991) 2228.
- [88] I. Kiricsi, H. Forster and G. Tasi, *Stud. Surf. Sci. Catal.* 46 (1989) 355.
- [89] K.V. Topchieva and S.A. Arystanbekova, *Vestn. Mosk. Univ. Ser. 2 Khim.* 23 (1982) 87.
- [90] M.E. Davis, C. Saldarriaga, C. Montes, J. Garces and C. Crowder, *Nature* 331 (1988) 698.
- [91] M.E. Davis, C. Montes, P.E. Hathaway, J.P. Arhancet, D.L. Hasha and J.M. Garces, *J. Am. Chem. Soc.* 111 (1989) 3919.
- [92] P.R. Rudolf and C.E. Crowder, *Zeolites* 10 (1990) 163.
- [93] L.B. McCusker, Ch. Bärlocher, E. Jahn and M. Bülow, *Zeolites* 11 (1991) 308.
- [94] P.J. Grobet, J.A. Martens, I. Balakrishnan, M. Mertens and P.A. Jacobs, *Appl. Catal.* 56 (1989) L21.
- [95] J.P. van B. Houckgeest, B. Kraushaar-Czarnetzki, R.J. Dogterom and A. de Groot, *J. Chem. Soc. Chem. Commun.* (1991) 666.
- [96] M. Stöcker, D. Akporiaye and K.-P. Lillerud, *Appl. Catal.* 69 (1991) L7.
- [97] L. Maistrau, Z. Gabelica and E.G. Derouane, *Appl. Catal.* 81 (1992) 67.
- [98] D. Akporiaye and M. Stöcker, *Zeolites* 12 (1992) 351.
- [99] J. Rocha, W. Kolodziejski, H. He and J. Klinowski, *J. Am. Chem. Soc.* 114 (1992) 4884.
- [100] H. He, W. Kolodziejski and J. Klinowski, *Chem. Phys. Lett.* 200 (1992) 83.
- [101] D. Goldfarb, H.-X. Li and M.E. Davis, *J. Am. Chem. Soc.* 114 (1992) 3690.
- [102] J.O. Perez, P.J. Chu and A. Clearfield, *J. Phys. Chem.* 95 (1991) 9994.